Cholecystokinin from the Rhinal Cortex Facilitates Motor Skill Learning

Hao Li [a,b], Jingyu Feng[a], Mengying Chen[a], Min Xin[a,b], Xi Chen[a], Kuan Hong Wang[c,*], Jufang He[a,b,*]

[a] *Departments of Neuroscience and Biomedical Sciences, City University of Hong Kong, China.*
[b] *Centre for Regenerative Medicine and Health, Hong Kong Institute of Science & Innovation, Chinese Academy of Sciences, China.*
[c] *Department of Neuroscience, Del Monte Institute for Neuroscience, University of Rochester Medical Center, USA.*

[*] **Correspondence at**: Jufang He, Email: jufanghe@cityu.edu.hk; Kuan Hong Wang, Email: kuanhong_wang@urmc.rochester.edu.

Author Contributions: Jufang He, Kuan Hong Wang, Hao Li and Jingyu Feng designed the research; Hao Li, Jingyu Feng, and Xi Chen set up behavior model and analysis methods; Hao Li, Mengying Chen and Min Xin carried out the experiments; Hao Li, Xi Chen, Jufang He and Kuan Hong Wang analyzed the data; Hao Li and Jufang He wrote the draft of the manuscript; Hao Li, Jufang He and Kuan Hong Wang edited the manuscript.

Keywords: Cholecystokinin, Entorhinal cortex, Motor cortex, Single pellet reaching task, Motor skill learning.

Abstract

Cholecystokinin (CCK) is an essential modulator for neuroplasticity in sensory and emotional domains. Here, we investigated the role of CCK in motor learning using a single pellet reaching task in mice. Mice with a knockout of *cck* gene ($CCK^{-/-}$) or blockade of CCK-B receptor (CCKBR) showed defective motor learning ability; the success rate of retrieving reward remained at the baseline level compared to the wildtype mice with significantly increased success rate. We observed no long-term potentiation (LTP) upon high-frequency stimulation (HFS) in the motor cortex of $CCK^{-/-}$ mice, indicating a possible association between motor learning deficiency and neuronal plasticity in the motor cortex. In vivo calcium imaging demonstrated that the deficiency of CCK signalling disrupted the refinement of population neuronal activity in the motor cortex during motor skill training. Anatomical tracing revealed direct projections from CCK-expressing neurons in the rhinal cortex to the motor cortex. Inactivating the CCK neurons in the rhinal cortex using chemogenetic methods significantly suppressed motor learning, and intraperitoneal application of CCK4, a tetrapeptide CCK agonist, rescued the motor learning deficits of $CCK^{-/-}$ mice. In summary, our results suggest that CCK, which could be provided from the rhinal cortex, enables neuroplasticity in the motor cortex leading to motor skill learning.

Introduction

Learning to perform motor skills is essential for survival and high quality of life, such as hunting, running, escaping, fighting, playing music, dancing, drawing, and performing an operation. Evidence from electrical stimulation, lesions, imaging, and more targeted manipulation shows that the motor cortex is the center that controls motor behaviors and motor skill learning in the brain (Papale and Hooks, 2018). Changes among neuronal circuits, such as synaptic strength, circuit connectivity, neuronal excitability, and neuronal structure, which occur through all layers of the motor cortex, contribute to motor skills learning (Papale et al., 2018; Biane et al., 2016; Peters et al., 2014; Costa et al., 2004; Huber et al., 2012). Different layers exhibit various neuronal changes with motor skill learning, corresponding with various layer-specific inputs and descending outputs. However, it is not completely clear how neuronal plasticity in the motor cortex is regulated.

Cholecystokinin (CCK), distributed throughout the whole brain, has been suggested to be important in neuronal plasticity (Li et al., 2014; Chen et al., 2019). Activation of the CCK-B receptor (CCKBR) by infusion of agonist in the auditory cortex regulated visuo-auditory associative memory formation in awake rats (Li et al., 2014). Projections from the entorhinal cortex of the medial temporal lobe release CCK in the neocortex, hippocampus, and amygdala, enabling the encoding of long-term associative, spatial, and fear memory (Li et al., 2014; Meunier et al., 1993, 1996; Chen et al., 2019; Su et al. 2019; Feng et al. 2021). NMDA receptors in the presynaptic membrane control the release of the entorhinal CCK in the auditory

cortex (Chen et al., 2019).

Motor memory, known as procedural memory, is quite distinct from declarative memory examined in previous studies of CCK functions, but both types involve neuronal changes in the neocortex caused by task training (Squire, 2004; Ackermann and Rasch, 2014). In the present study, we investigated the role of CCK from the rhinal cortex, including the entorhinal cortex and perirhinal cortex, to the motor cortex in neuroplasticity and motor skill learning. We examined whether the motor learning ability of mice is affected by the genetic elimination of *cck* gene or the administration of the CCKBR antagonist. We adopted calcium imaging of the motor cortex to verify whether the absence of CCK function disrupts the refinement of the neuronal activation pattern during motor training. We further examined immunohistochemically the CCK-positive neuronal projections from the rhinal cortex to the motor cortex, including the laminar specificity of these projections in their target regions. In the final set of behavioral studies, we examined whether the loss-of-function by inactivating CCK neurons in the rhinal cortex suppresses motor learning ability and the gain-of-function by CCK4 administration rescues the motor learning ability of $CCK^{-/-}$ mice.

Results

The role of CCK in motor learning

A previous study showed that CCK is a key factor regulating neuronal plasticity that enhances long-term memory formation in the auditory cortex (Chen et al., 2019).

Therefore, we introduced a single pellet reaching task to train transgenic $CCK^{-/-}$ mice and their wildtype control (C57BL/6) to use the dominant forelimbs and obtain food rewards as the method to determine whether CCK is involved in motor learning (Figure 1A). This task, including shaping and training, has been adopted in many studies on motor skill learning and motor control systems, especially those controlling the forelimb (Figure 1B) (Xu et al., 2009; Wang et al., 2017). The performance of wildtype and $CCK^{-/-}$ mice was evaluated based on the success rate, which requires accurate performance in aiming, reaching, grasping, and retrieval (Video 1). The success rate of $CCK^{-/-}$ mice did not increase after six days of training, remaining at the baseline level of approximately 15% (Figure 1C, Figure S1; $CCK^{-/-}$ mice, one-way RM ANOVA, $F[5,35] = 0.574$; $p = 0.72$; post hoc. pairwise comparison between different days, Day 1 vs. Day 3, 15.05% ± 4.40% vs. 11.91% ± 3.60%, $p = 0.59$; Day 1 vs. Day 6, 15.05% ± 4.40% vs. 15.59% ± 3.36%, $p = 0.924$), while wildtype mice performed much better, of which the success rate increased significantly to 30.94% on day 3 and remained at a plateau until the end of training (Figure 1C; WT mice, one-way RM ANOVA, $F[5,45] = 4.904$; $p < 0.001$; post hoc. pairwise comparison, Day 1 vs. Day 3, 14.63% ± 3.05% vs 30.94% ± 4.17%, $p = 0.013 < 0.05$; Day 1 vs Day 6, 14.6% ± 3.05% vs. 32.76% ± 3.12%, $p = 0.004<0.01$; between WT and $CCK^{-/-}$ mice, two-way mixed ANOVA, significant interaction, $F[5,80] = 4.03$, $p = 0.003 < 0.01$; post hoc. comparison bewteen two groups, $F[1,16] = 7.697$, $p = 0.014 < 0.05$; WT vs. $CCK^{-/-}$, Day 3, 30.94% ± 4.17% vs. 11.91% ± 3.60%, $F[1,16] = 11.239$, $p = 0.004 < 0.01$; Day 4, 28.96% ±

120 2.90% vs.17.37% ± 4.35%, $F[1,16] = 5.266$, $p = 0.036 < 0.05$; Day 5, 31.90% ±
121 3.50% vs.16.56% ± 4.51%, $F[1,16] = 7.465$, $p = 0.015 < 0.05$; Day 6, 32.76 % ±
122 3.12% vs. 15.59% ± 3.36%, $F[1,16] = 13.906$, $p = 0.0018 < 0.01$). The success rates
123 of wildtype and $CCK^{-/-}$ mice were similar on day one, indicating that CCK did not
124 affect the basic ability to carry out the task, although the learning ability was inhibited
125 (Figure 1C; t-test, WT vs. $CCK^{-/-}$, 14.62% ± 3.05% vs. 15.05% ± 4.40%, $p = 0.9366$).
126 We also evaluated the variation of trajectories of the hand movement. The deviation
127 of the trajectories of different trials of a wildtype mouse became visibly smaller on
128 Day 3 compared with that on Day 1, while that of a $CCK^{-/-}$ mouse showed no visible
129 improvement (Figure 1D). We calculated the Hausdorff distances, the greatest of all
130 the distances from a point in one set to the closest point in the other set, to evaluate
131 the variation of trajectories (Aydin et al.,2021). The Hausdorff distance for the
132 trajectories of wildtype and $CCK^{-/-}$ mice are similar at Day 1 (Figure 1E; t-test, WT vs.
133 $CCK^{-/-}$, 0.53 ± 0.04 cm vs. 0.50 ± 0.04 cm, $p = 0.5908$). However, after 3 days'
134 training, the Hausdorff distance for wildtype mice significantly decreased while
135 $CCK^{-/-}$ mice remained unchanged (Figure 1E; paired t-test, WT, Day 1 vs. Day 3, 0.53
136 ± 0.04 cm vs. 0.42 ± 0.02 cm, $p = 0.003 < 0.01$; $CCK^{-/-}$, Day 1 vs. Day 3, 0.50 ± 0.04
137 cm vs. 0.48 ± 0.03 cm, $p = 0.514$).

138 Failures in retrieving the pellets, including miss, no-grasp, and dropping, are also
139 applied to assess specific learning defects in different movement phases of the
140 complex task, comprising the deficiency of "success", which only indicates the final
141 execution results (Figure 1F). "Miss", representing no touching of the food pellet in

142 front of the wall of the chamber, is due to inaccurate aiming and inadequate
143 preparation of the neuronal system, especially processes involved in motor control
144 and execution (Video 2). A "no-grasp" is a reach in which the mouse shows a defect in
145 finger closure around food pellets for retrieval (Video 3). A "drop" is a reach in which
146 the mouse drops the food pellet before putting it into the mouth, although the pellet
147 was grasped correctly, indicating a defect in neurons controlling the retrieval process
148 (Video 4). The miss rate of $CCK^{-/-}$ mice was higher than that of wildtype mice,
149 suggesting that CCK may affect the learning ability in aiming and preparing to
150 execute a motor task (Figure 1G; paired t-test, WT, Day 1 vs. Day 6, 32.54% ± 6.43%
151 vs. 11.62% ± 3.58%, $p = 0.0127 < 0.05$; $CCK^{-/-}$, Day 1 vs. Day 6, 30.77% ± 7.07 % vs.
152 22.25% ± 2.09%, $p = 0.1732$; t-test, WT vs. $CCK^{-/-}$, Day 6, 11.62% ± 3.58% vs.
153 22.25% ± 2.09%, $p = 0.0265 < 0.05$).

154 Further, we conducted an electrophysiology experiment on the slices of the motor
155 cortex from wildtype and $CCK^{-/-}$ mice to investigate the potential physiological causes
156 for the defects in motor skill learning of $CCK^{-/-}$ mice. We observed LTP in field
157 excitatory postsynaptic potential (fEPSP) after HFS in the wildtype mice, but no LTP
158 from $CCK^{-/-}$ mice, suggesting that CCK plays a key role in neuronal plasticity in the
159 motor cortex (Figure 1H, 1I; two-way mixed ANOVA, $F[1,24] = 3.154$, $p = 0.088$;
160 post hoc. pairwise comparison, WT, before vs. after HFS, 100.06% ± 0.35% vs.
161 134.38% ± 8.61%, $F[1,20] = 17.255$, $p < 0.001$; $CCK^{-/-}$, before vs. after, 99.82% ±
162 0.48% vs. 104.62% ± 7.99%, $F[1,6] = 0.5$, $p = 0.506$).

163 In summary, $CCK^{-/-}$ mice showed an impaired ability in motor skill learning in the

single pellet reaching task and a defect in the LTP induction in the motor cortex.

A CCKBR antagonist injection in the motor cortex inhibited the motor learning ability of C57BL/6 mice

As deletion of the *cck* gene in the $CCK^{-/-}$ is general, the above experiment results could not indicate the source of CCK and their action site in the brain. We limited our manipulation of the CCK signaling in the motor cortex, targeting its primary receptor, CCKBR, in the neocortex. We have implanted a drug infusion cannula into the motor cortex contralaterally to its dominant forelimb and injected the CCKBR antagonist, L365,260 or its vehicle control to examine whether blocking the CCKBRs in the motor cortex could affect motor skill learning (Figure 2A).

We infused L365.260 to the experimental group or vehicle (ACSF + 0.1% DMSO) to the control group through the implanted drug cannula in the motor cortex every day before training. The success rate of pellet retrieval of the experimental group was not improved through the 6-day training period (Figure 2B, Figure S2A; one-way RM ANOVA, $F[5,50] = 1.959$, $p = 0.101$), while that of the vehicle control group was significantly improved to 32.30% at Day 3 and kept at this level till the end of training (Figure 2B, Figure S2B; one-way RM ANOVA, pairwise comparison, Day 1 vs. Day 3, 19.02% ± 4.27% vs. 32.30% ± 3.62%, $F[1,10] = 5.628$, $p = 0.039 < 0.05$; Day 3 vs. Day 6, 32.30% ± 3.62% vs. 32.90% ± 7.07%, $F[1,10] = 0.007$; $p = 0.937$). The differences in the success rate between the experimental and control groups were significant (Two-way mixed ANOVA, $F[5,70] = 1.881$, $p = 0.109$; post hoc.

comparison between Antagonist and Vehicle, $F[1,14] = 5.066$, $p = 0.041$; Day 3, Antagonist vs. Vehicle, $16.80 \pm 2.83\%$ vs. $32.30 \pm 3.62\%$, $F[1,15] = 11.266$, $p = 0.0048 < 0.01$; Day 4, $18.16 \pm 3.12\%$ vs. $32.90 \pm 5.03\%$, $F[1,15] = 6.876$, $p = 0.019 < 0.05$). This result suggests that CCK participates in motor skill learning by regulating neuronal plasticity in the motor cortex.

For the detailed reaching results, we compared the performance of the experimental and control groups on Day 1 and Day 5. The number of "miss" of the antagonist group had no significant decrease with learning, but for the vehicle group, it dropped from 35% to 10%, indicating that the aiming and advance learning abilities were significantly impaired by inactivation CCKBRs in the motor cortex (Figure 2C, paired t-test, Antagonist, Day 1 vs. Day 5, $27.34\% \pm 9.85\%$ vs. $24.75\% \pm 2.34\%$, $p = 0.794$; Vehicle, Day 1 vs. Day 5, $33.05\% \pm 6.68\%$ vs. $9.17\% \pm 6.04\%$, $p = 0.044 < 0.05$). For the "no-grasp" outcome, the vehicle group increased significantly by 12.24%, indicating that the implantation of a cannula may cause injury to the motor cortex, leading to defects in digit learning (Figure 2C; paired t-test, "no-grasp" , Day 1 vs. Day 5, $26.49\% \pm 3.26\%$ vs. $38.73\% \pm 4.05\%$, $p = 0.017 < 0.05$), while that of antagonist showed no improvement increase (Paired t-test, "no-grasp", Day 1 vs. Day 5, $33.78\% \pm 3.36\%$ vs. $34.69\% \pm 4.12\%$, $p = 0.85$). The drop rate of both groups had no significant changes, indicating that the retrieval learning ability was not affected (Figure 2C). In summary, CCK plays a critical role in memory acquisition by activating the CCK receptors in the motor cortex at the overall level.

208 ***Calcium imaging of layer 2/3 of the motor cortex during motor skill learning***

209 Based on the outcome of the above drug infusion experiment and previous studies,
210 the motor cortex is one of the primary sites for motor skill learning (Wang et al.,
211 2017). Previous studies found that neuronal activity patterns in the Layer 2/3 of the
212 motor cortex were refined, exhibiting reproducible spatiotemporal sequences of
213 activities with motor learning (Peters et al., 2014). Therefore, calcium imaging of
214 neurons in the motor cortex layer 2/3 of C57BL/6 mice, $CCK^{-/-}$ mice and C57BL/6
215 mice injected with the CCKBR antagonist was performed to determine the activities
216 of neurons in the motor cortex during the single pellet reaching task.

217 We hypothesized that the CCK-enabled neuronal plasticity happens at the
218 population level in the motor cortex. To test the hypothesis, we attached a one-photon
219 miniscope over the motor cortex, contralateral to the dominant hand of the mouse,
220 with an implanted high light transmission glass window in between (Figure 3B). We
221 installed a web camera in front of the training chamber to simultaneously monitor the
222 mouse performing the task with the neuronal activities.

223 We recruited three groups of mice, 1) C57BL/6, 2) $CCK^{-/-}$, and 3) C57BL/6 with
224 CCKBR antagonist, to examine how CCK signaling affects neuronal activities in the
225 motor cortex (Figure 3A). We first confirmed GCaMP6s signals in layer 2/3 of the
226 motor cortex, as shown in the examples (Figure 3B; Video 5). The neuronal signals
227 were extracted with CNMF-E and analyzed with MATLAB (Figure 3C). Neurons
228 showed various temporal and spatial responses to the movements during the task.

229 The neuronal activity pattern, excluding the indiscriminate neurons (ranksum test,
230 neuronal activity during reaching & not reaching, $p \geqslant 0.05$), in the C57BL6 group,

231 was refined after six days of training; the peak activity of the neurons became stronger
232 with lower background activity (Figure 3D). These results are similar to that of layer
233 2/3 neurons of the motor cortex in a mouse performing a lever-press task (Peters et al.,
234 2014). In contrast, we found no apparent changes after training for six days for groups
235 of $CCK^{-/-}$ and C57BL/6 mice injected with the antagonist, the neuronal activity
236 pattern (Figure 3D).

237 The population activity of neurons varied with time relative to movement onset,
238 starting to rise around 0.2 s before movement onset and reaching the peak at the time
239 of 0.33 s after movement onset (Figure 3E and Figure S3). The activated population
240 activity, peak activity minus baseline activity, for C57BL/6 mice increased
241 significantly with training (Figure 3F; paired t-test, Day 1 vs. Day 6, 0.0216 ± 0.0062
242 vs. 0.0593 ± 0.0114, $p = 0.044 < 0.05$). However, we observed no significant change
243 in the activated population activity for both $CCK^{-/-}$ and L365,260 groups (Figure 3F;
244 paired t-test, $CCK^{-/-}$, Day 1 vs. Day 6, 0.0313 ± 0.0057 vs. 0.0386 ± 0.0099, $p = 0.237$;
245 L365,260, Day 1 vs. Day 6, 0.0218 ± 0.0094 vs. 0.0354 ± 0.0080, $p = 0.240$).

246 We adopted the Pearson correlation coefficient to evaluate the recurrence of
247 neuronal activities among reaching trials. We compared the average correlation
248 coefficient of neuronal activities of different trials between Day 1 and Day 6. We
249 observed a significant increase in the trial-to-trial population activity correlation on
250 Day 6 compared with Day 1 in the C57BL/6 mice group (Figure 3G, one-way RM
251 ANOVA, Day 1 vs. Day 6, 0.023 ± 0.01 vs. 0.12 ± 0.04, $F[1,9] = 5.342$, $p = 0.046 <$
252 0.05). However, we observed no significant differences in the correlations between

Day 1 and Day 6 in the $CCK^{-/-}$ group, nor in the L365,260 group (Figure 3G; one-way RM ANOVA, $CCK^{-/-}$, Day 1 vs. Day 6, 0.10 ± 0.07 vs. 0.07 ± 0.06, $F[1,6] = 0.073$, $p = 0.796$; L365/260, Day 1 vs. Day 6, 0.12 ± 0.07 vs. 0.12 ± 0.05, $F[1,6] = 0.005$, $p = 0.944$). The pairwise Hausdorff distance of trajectories in C57BL/6 group decreased significantly with training, while no significant changes were observed in $CCK^{-/-}$ or L365,260 injection group, suggesting that the population activities are in line with the changes of the variation of the trajectories during motor learning (Figure 3H; paired t-test, C57BL/6, Day 1 vs. Day 6, 0.6613 ± 0.017 cm vs. 0.5588 ± 0.0227 cm, $p = 0.0075 < 0.01$; $CCK^{-/-}$, Day 1 vs. Day 6, 0.6787 ± 0.0470 cm vs. 0.6760 ± 0.0501 cm, $p = 0.9219$; L365,260, Day 1 vs. Day 6, 0.7012 ± 0.0594 cm vs. 0.6712 ± 0.0659 cm, $p = 0.5606$). The trial-to-trial population activity correlation in L365,260 group on Day 1 appeared to be higher than that in C57BL/6 group. This might be due to that the drug blocked the trial-to-trial learning on Day 1, suppressing the exploration of the optimal path and abandonment of bad movements that would otherwise occur in wildtype mice.

Taken together, CCK deficiency causes defects in neuronal refinement and the reproducibility of neuronal activity among different trials during motor skill learning.

CCK-expressing neurons in the lateral entorhinal cortex projecting to the motor cortex

Our next quest was to find what CCK projection is crucial in motor skill learning. We understand that CCK neurons in the entorhinal cortex, a gateway from the

hippocampus to the neocortex, play critical roles in encoding sound-sound, visuoauditory, fear, and spatial memory (Li et al, 2014; Chen et al, 2019; Feng et al, 2021; Su et al. 2019). These findings prompted us to examine whether CCK-expressing neurons in the entorhinal cortex also project to the motor cortex.

We used both anterograde and retrograde viruses to track neuronal projections in this study. We first injected a Cre-dependent, highly efficient AAV virus expressing mCherry into the rhinal cortex of one hemisphere of 8-week-old CCK Cre mice (Figure 4A). This viral vector is expected to be taken up in the soma of neurons and transported to the axon terminus. In the motor cortex, mCherry-expressing neuronal axons mainly spread in layer 2/3 or layer 6 (Figure 4B). We next injected A Cre-dependent retrograde AAV vector expressing EYFP fluorescent protein gene into the motor cortex in deep layers and superficial layers to verify the projections from the lateral entorhinal cortex to the motor cortex (Figure 4C). In the rhinal cortex, the EYPF-labeled soma spread from AP: -2.54 to AP: -4.30, and local clusters were observed in layer 4 and layer 5, where the neurons are expected to project to the neocortex (Figure 4D). Both anterograde and retrograde tracking results indicated that CCK-expressing neurons in the rhinal cortex projecting to the motor cortex were asymmetric, showing a preference for the ipsilateral hemisphere. Primary antibodies against GAD67 and CaMK2a were used for the immunostaining of the rhinal cortex sections to determine the characteristics of CCK neurons projecting to the motor cortex. None of the retrograde EYFP-labeled neurons merged with GAD67 staining but completely colocalized with CaMK2a staining, indicated by the white arrowhead,

297 suggesting that the neurons projecting to the motor cortex are all excitatory neurons
298 (Figure 4E and 4F). Therefore, CCK neurons in the rhinal cortex may affect motor
299 skill learning by regulating the plasticity of neurons in the motor cortex.
300
301 ***Inhibiting CCK neurons in the EC/PC suppresses motor learning***
302 In the following experiment, we adopted chemogenetics to selectively silence the
303 CCK projection neurons from the rhinal cortex to the motor cortex to examine their
304 involvement in motor skill learning.
305 We injected a Cre-dependent AAV vector carrying hM4Di or mCherry into the
306 rhinal cortex bilaterally in CCK-Cre mice one month before the behavior test (Figure
307 5A). Clozapine was intraperitoneally injected, followed by an approximately 30 min
308 period for drugs to be taken up and transported to the brain. The drug bound to the
309 hM4Di and inactivated the neurons (Figure 5A). The success rate of hM4Di with the
310 clozapine injection group showed no significant increase after six days of training,
311 while the success rate of the control group of mCherry with clozapine injection
312 increased significantly beginning on the third day of training and remained at a high
313 level until the end of training (Figure 5B, Figure S4A, S4B; hM4Di+Clozapine group,
314 one-way RM ANOVA, $F[5,50] = 0.839$, $p = 0.528$; mCherry+Clozapine group,
315 one-way RM ANOVA,,$F[5,35] = 3.121$, $p = 0.02 < 0.05$; two-way mixed ANOVA,
316 post hoc. comparison between two groups, $F[1,17] = 7.014$, $p = 0.016 < 0.05$, hM4Di
317 vs. mCherry, Day 3, 12.92% ± 3.10% vs. 25.99% ± 3.62%, $F[1,17] = 7.510$, $p = 0.014$
318 < 0.05; Day 4, 12.04% ± 1.84% vs. 24.78% ± 3.34%, $F[1,17] = 12.804$, $p = 0.002 <$

319 0.01; Day 5, 15.02% ± 2.55% vs. 25.74% ± 3.72%, $F[1,17] = 6.061$, $p = 0.025 < 0.05$;
320 Day 6, 14.41% ± 4.01% vs. 28.42% ± 5.64%, $F[1,17] = 4.354$, $p = 0.052$.).

321 To exclude the possibility that hM4Di alone might regulate the neurons in this
322 system, we administered saline as the control to the mice with the same virus vector
323 with hM4Di injected into the rhinal cortex of CCK-Cre mice, as compared to the
324 clozapine-administered experimental group (Figure 5A). The learning curve of the
325 control group injected with saline showed a learning trend in the single pellet reaching
326 task, similar to the "mCherry + clozapine" group, and the success rate was
327 significantly different from the "hM4Di+clozapine" group (Figure 5C, Figure S4C;
328 hM4Di + saline group, one-way RM ANOVA, $F[5,45] = 7.911$, $p < 0.001$; between
329 groups, two-way mixed ANOVA, significant interaction, $F[5,95] = 2.813$, $p = 0.021 <$
330 0.05, hM4Di+saline vs. hM4Di+clozapne, post hoc. comparison between two groups,
331 $F[1,19] = 6.193$, $p = 0.022 < 0.05$; post hoc. comparison between two groups on
332 different days, Day 3, 24.02% ± 3.93% vs. 12.12% ± 3.10%, $F[1,19] = 5.013$ $p =$
333 $0.0373 < 0.05$; Day 4, 27.81% ± 3.84% vs. 12.04% ± 1.84%, $F[1,19]= 14.534$, $p =$
334 $0.0012 < 0.01$; Day 5, 24.54% ± 3.05% vs. 15.02% ± 2.55%, $F[1,19] = 5.785$, $p =$
335 $0.0263 < 0.05$; Day 6, 30.60% ± 4.59% vs. 14.41 ± 4.01%, $F[1,19] = 7.128$, $p =$
336 $0.0151 < 0.05$; The hM4Di+clozapine curve in Figure 5C shared that in Figure 5B).
337 These results concluded that CCK neurons in the rhinal cortex may be crucial for
338 motor learning.

339

340 ***Rescue of the motor learning ability of the CCK$^{-/-}$ mice with CCK4***

So far, we have examined the potential involvement of CCK in motor skill learning with several loss-of-function studies. We next designed a gain-of-function experiment to see whether CCKBR agonist could rescue the defective motor learning ability. A tetrapeptide, CCK4 (Trp-Met-Asp-Phe-NH2), a CCKBR agonist that can pass through the brain-blood barrier, was chosen to regain the defective motor learning ability of $CCK^{-/-}$ mice (Feng et al., 2021).

Firstly, we examined whether CCK4 could rescue the defective neuronal plasticity in the motor cortex of $CCK^{-/-}$ mice. We carried out electrophysiology recording on the motor cortex of the brain slices from the $CCK^{-/-}$ mice. After 15 minutes of stable baseline recording, CCK4 or vehicle was injected into the electrode dish and applied HFS, followed by 60 minutes of recording. We observed a significant rescuing effect by CCK4 application before the HFS compared with its vehicle control (Figure 6A and 6B; Vehicle vs. CCK4, two-way mixed ANOVA, significant interaction during -10 - 0 min and 50-60 min, $F[1,21] = 10.656$, $p = 0.004 < 0.01$; post hoc. comparison between two groups, $F[1,21] = 7.997$, $p = 0.01 < 0.05$; Vehicle, before vs. after, $100.95\% \pm 0.67\%$ vs. $95.53\% \pm 5.77\%$, $F[1,10] = 1.239$, $p = 0.292$; CCK4, before vs. after, $100.28\% \pm 0.47\%$ vs. $118.89\% \pm 6.09\%$, $F[1,11] = 11.653$, $p = 0.006 < 0.01$).

Next, we examined whether the CCK4 application could rescue the motor skill learning of $CCK^{-/-}$ mice. We injected with CCK4 or vehicle solution intraperitoneally to $CCK^{-/-}$ mice every day before the 6-day training (Figure 6C). The success rate of CCK4-injected group kept at the baseline level in the first three days and started to increase gradually from Day 4 to Day 6 (Figure 6D, Figure S5A; CCK4, one-way RM

363 ANOVA, $F[5,50] = 3.914$, $p = 0.005 < 0.01$; Day 5 vs. Day 1, 30.58% ± 4.18% vs.
364 19.17% ± 3.03%, $F[1,10] = 5.680$, $p = 0.038 < 0.05$; Day 6 vs. Day 1, 31.50% ±
365 4.43% vs. 19.17% ± 3.03%, $F[1,10] = 6.893$, $p = 0.025 < 0.05$;). In contrast, we
366 observed no improvement in the success rate in the vehicle control group mice
367 (Figure 6D, Figure S5B; Vehicle, one-way RM ANOVA, $F[5,55] = 0.476$, $p = 0.793$).
368 The between-group comparison showed that the CCK4 group had significantly higher
369 success rate from Day 5 to Day 6 compared to the vehicle group (Figure 6D; Vehicle
370 vs CCK4, two-way mixed ANOVA, significant interaction, $F[5,105] = 2.405$, $p =$
371 $0.043 < 0.05$; post hoc. comparison between Vehicle and CCK4, Day 5, 14.88% ±
372 2.61% vs. 30.51% ± 4.18%, $F[1,21] = 10.459$, $p = 0.004 < 0.01$; Day 6, 17.76% ±
373 3.25% vs. 31.50% ± 4.43%; $F[1,21] = 6.412$, $p = 0.019 < 0.05$).

374 We compared the detailed reaching results on Day 1 and Day 5 between the CCK4
375 and the vehicle groups. We found the miss rate of the CCK4 group dropped
376 significantly at Day 5 compared to Day 1, while that of the vehicle group showed no
377 significant change (Figure 6E; paired t-test, Vehicle, Day 1 vs Day 5, 26.12% ± 5.71%
378 vs. 18.71% ± 4.31%; $F[1,11] = 1.155$, $p = 0.305$; CCK4, Day 1 vs Day 5, 25.47% ±
379 4.03% vs. 13.13% ± 2.80, $F[1,10] = 6.643$, $p = 0.028 < 0.05$), suggesting that the
380 CCK4 rescued the aiming in reaching. This result demonstrated that CCK4 could
381 cross the brain blood barrier and partially rescue the motor learning ability of $CCK^{-/-}$
382 mice (Figure 6E).

383 Therefore, CCK is the crucial signal that enables motor learning. Intraperitoneal
384 injection of CCK4 is sufficient to rescue the motor learning ability by turning on the

385 neuronal plasticity of the CCK$^{-/-}$ mice.

386

387 **Discussion**

388 CCK$^{-/-}$ mice showed defective motor learning ability, of which the success rate of
389 retrieving reward remained at the baseline level compared to the wildtype mice with a
390 significantly increased success rate. We induced no LTP by HFS in the motor cortex
391 of CCK$^{-/-}$ mice but readily in their wildtype control, indicating a possible association
392 between the motor learning deficiency and neuronal plasticity in the motor cortex. *In*
393 *vivo* calcium imaging demonstrated that the deficiency of CCK signaling led to the
394 defect in the population neuronal plasticity in the motor cortex affecting motor skill
395 learning.

396 We found that the CCK-positive neurons in the rhinal cortex projected to the motor
397 cortex, using both anterograde and retrograde tracing methods. Inactivating the CCK
398 neurons in the rhinal cortex using chemogenetic methods significantly suppressed the
399 motor learning ability. Our further gain-of-function study revealed that intraperitoneal
400 application of CCK4 rescued the defective motor skill learning of CCK$^{-/-}$ mice.

401 Neuronal plasticity of the motor cortex has been assessed by many researchers
402 using multiple methods, such as single pellet reaching task and lever-press task (Xu et
403 al., 2009; Peters et al., 2014). Other brain areas are also involved in motor skills
404 learning, such as thalamus, striatum, cerebellum, and midbrain. Thalamocortical
405 projections in the motor cortex are widely distributed in all layers, including inputs to
406 corticospinal neurons in layer 5 (Hooks et al., 2013). With single pellet reaching task
407 training, thalamocortical neurons are biased in activating the corticospinal neurons

that control the performance of the task, though the unbiased activation of corticospinal neurons was observed before training, suggesting that the thalamus selectively activates corticospinal neurons to generate better control of the forelimb movement with motor learning (Biane et al., 2016). The spiking of Purkinje neurons switched from more autonomous, the baseline condition, to time-locked activation or silence before reaching onset to produce a state promoting a high quality of movement, as mice learn to direct a robotic manipulation toward a target zone (Wangner et al., 2021). The ventral tegmental area (VTA) dopaminergic projection in the motor cortex is necessary for motor skill learning but not for execution. The VTA projection to the motor cortex may facilitate the encoding of a motor skill memory by relaying food reward information related to the task (Hosp et al., 2011). As the core area where dexterous motor memory is encoded, the plasticity of the motor cortex enables animals to learn complex motor tasks.

CCK produced in the rhinal cortex has been identified as the key to transforming a paired tone into auditory memory in mice and rats by regulating the plasticity of neurons in the auditory cortex (Li et al., 2014). In the present study, we found that genetic knockout of the *cck* gene caused defects in motor learning, while the success rate of wildtype mice increased to 30.94% on day 3. The success rate alone is not sufficient to describe the function of CCK in motor skill learning; therefore, the reaching result of the task is divided into four types, "miss", “no-grasp”, “drop” and “success”. “Miss” is caused by defects in “aiming” and “advance”, indicating a low probability of hitting the pellet. Miss rate of the $CCK^{-/-}$ mice decreased with learning

but showed less improvement than the wildtype mice, suggesting that the brain areas controlled the "aiming" and "advance" are affected by CCK partially. Besides, "no-grasp" and the "success" rate of $CCK^{-/-}$ mice remained at the same levels after training, but the "drop" rate increased, suggesting that the improved "miss" trials finally turned to "drop". The variation of the trajectories of the $CCK^{-/-}$ mice is lower than that of the wildtype mice on the first day, which is consistent with the previous results that the animals with low variation in trajectories learn worse than those with wide variation in trajectories at the initiation stage (Wu et al., 2014). The reason may be that when animals perform a motor task, the wider the variation of the movement, the easier it is for the mice to find the best path to complete the task. The lack of CCK impaired the plasticity of neurons in the motor cortex, which is deemed the basis for motor learning.

The motor cortex plays the leading role in controlling motor memory encoding (Cheney, 1985; Sanes and Donoghue, 2000; Economo et al., 2018; Svoboda and Li, 2018). CCKBRs dominate CCKARs in the neocortex including the motor cortex (Crawley and Corwin, 1994; Wank, 1995). Blockade of the CCKBRs in the motor cortex suppressed the improvement in the success rate of mice in the single pellet reaching task (Figure 2B). The gradually improved success rate on Day 5 and 6 (Figure 2B) after CCKBR antagonists could be due to the lasting of the antagonists was not long enough to cover the whole training period, partially due to the diffusion of the antagonist. The performance of both the "antagonist" and "vehicle" groups was similar on the first day, indicating a similar neuronal baseline condition for each group.

452 Activating CCKBR by CCK agonist improves motor skill learning.

453 Based on the evidence that CCK is important for neuronal plasticity of the motor
454 cortex and motor skill learning, the next question is how CCK affects the changes in
455 neuronal activity of the motor cortex during training. An earlier study found that
456 neuronal activities in layer 2/3 of the motor cortex were modified, exhibiting more
457 reproducible spatiotemporal sequences of neuronal activities with motor learning
458 (Peters et al., 2014).

459 In the present study, the neuronal activities related to the task in layer 2/3 of the
460 motor cortex of C57BL/6 mice were refined with motor skill learning, the activation
461 of neurons becoming more reproducible among trials. The reproducibility changes of
462 neural activities are in parallel with the reduced variations in the trajectories of the
463 C57BL/6 mice after training (Figure 1F, 1G). However, $CCK^{-/-}$ mice generated
464 distinct changes in the neuronal activity in the motor cortex compared with C57BL/6
465 mice. The pattern of the peak activity and the trial-to-trial population correlation had
466 no significant differences after six days of motor learning, suggesting no refinement
467 in the neuronal circuit after motor learning in $CCK^{-/-}$ mice (Figure 3D).

468 In order to exclude a different background of neuronal activity due to long-term
469 accommodation to the lack of CCK in $CCK^{-/-}$ mice, we injected the CCKBR
470 antagonist, L365,260 into the motor cortex of C57BL/6 mice and observed no
471 significant changes in the pattern of the peak activity and the trial-to-trial population
472 correlation had after six days of motor learning, similarly to the $CCK^{-/-}$ mice.

473 The entorhinal cortex is crucial for learning and memory (Chen et al., 2013; Feng et

al 2021). Our group found that CCK is essential for neuronal plasticity in the auditory cortex (Li et al., 2014). In this research, we determined that CCK from the rhinal cortex may be critical for motor skill learning.

In the rhinal cortex, CCK-positive neurons that project to motor cortex are excitatory neurons (Figure 4E, 4F). The roles of both CCK and glutamate in the neuronal plasticity and the relationship between CCK and glutamate have been studied before (Bandopadhyay and Belleroche, 1991; Chen et al., 2019). In the previous study, we found that CCK is critical for HFS induced LTP, and CCK release is triggered by the activation of (N-methyl-D-aspartate) NMDA receptors that could be located in the presynaptic membrane of CCK-positive neurons (Chen et al., 2019). In the motor cortex, many CCK-positive neurons are GABAergic (γ-aminobutyric acid) neurons, in which the role CCK played is not very clear. However, evidence showed that GABA may inhibit the release of CCK in the neocortex (Yaksh et al., 1987). Many glutamatergic neurons in the neocortex also express CCK (Watakabe et al., 2012). Future study in the future is needed to investigate the role of cortical CCK-positive neurons, including inhibitory and excitatory neurons, played in neuronal plasticity and motor skill learning.

The hippocampus system, including the rhinal cortex, plays an essential role in declarative learning based on the finding of the famous patient H.M. (Corkin, 1968). However, the understanding of the role of the hippocampus system in motor skills learning is not consistent (Corkin, 1968; De et al., 2019). In the mirror tracking task, the performance of H.M. was on par with normal people, suggesting that the motor

learning ability was not affected without the hippocampus system (Corkin, 1968). But in the other two motor learning tasks, rotary pursuit and bimanual tracking, the performance of H.M. was much worse than the control. Besides, the movement of H.M. was slower when performing the task. This explanation is not enough to exclude the effects of the hippocampus system on motor skill learning. Indeed, Corkin herself thought that the H.M. could perform tasks that required less demanding motor skills, but not the tasks demanding better motor skills (Corkin, 1968; Brigard, 2019).

The single pellet reaching task is a complex and dexterous motor task requiring the neocortex and the whole motor system. Chemogenetic inactivation of CCK neurons in the rhinal cortex significantly impaired the mice's motor learning ability compared to the two control groups.

Based on the anterograde and retrograde tracing of the neurons in the rhinal cortex, projections terminals from the rhinal cortex to the motor cortex were distributed to the superficial and deep layers (Figure 4B, 4D). Previous research on both layer 2/3 and layer 5 found that motor skill learning refined neuronal activity in layer 2/3 of the motor cortices of the mice in a lever-press task. Thus, the CCK projections in the superficial layer may be where plasticity occurs (Peters et al., 2017; Heindorf et al., 2018). Two-photon calcium imaging results from previous research indicated that spine generation and elimination occurred in the apical dendrites (in the superficial layer) of neurons in layer 2/3. Still, the spines around the soma of the neurons in layer 2/3 showed no significant changes (Chen et al., 2015), consistent with the location of CCK neuron terminals projecting from the rhinal cortex.

518 Therefore, CCK from the rhinal cortex promotes dexterous motor skill learning by
519 regulating the activity of the motor cortex.

520

521 **Rescuing Neuroplasticity and Motor Skill Learning**

522 Our gain-of-function experiment by injecting CCK4 to rescue the defective
523 learning ability of $CCK^{-/-}$ mice supported the critical role of CCK in neuronal
524 plasticity of the motor cortex and motor skill learning. The CCKBRs of $CCK^{-/-}$ mice
525 were not influenced by knocking out the *cck* gene, making it possible that the
526 exogenous CCK activates the CCKBRs (Feng et al., 2021). CCK4, a tetrapeptide, can
527 pass through the blood-brain barrier. $CCK^{-/-}$ mice with the defective motor learning
528 capability improved significantly after the daily, single intraperitoneal injection of
529 CCK4, to a comparable level as their wildtype control at Day 5. The results of the
530 rescuing experiment imply a potential new target for facilitating motor rehabilitation.

531

532 **Materials and Methods**

533 ***Animal***

534 Young adult wildtype (C57BL/6) mice and C57BL/6 background transgenic mice,
535 CCK-Cre (CCK-ires-Cre, Stock #012706, Jackson Laboratory) and $CCK^{-/-}$
536 (CCK-CreER, strain #012710, Jackson Laboratory), were used for behavior,
537 electrophysiology and anatomy experiments. All mice were housed in the
538 pathogen-free 12 hours light/dark cycle holding room with the temperature at 20 - 24
539 ^{o}C. All experimental procedures were approved by the Animal Subjects Ethics Sub-

Committee of the City University of Hong Kong.

Single pellet reaching task

The behavioral experiment, single pellet reaching task, was modified based on a previously established procedure (Xu et al., 2009; Chen et al., 2014). A clear and transparent Plexiglas chamber (5 mm thickness, dimensions 20 cm x 15 cm x 8.5 cm) was built for mice training, with three 5 mm wide slits on the front wall; one is in the middle, the other two are 1.9 cm to the side, respectively. A 1.0-cm-height exterior shelf was affixed in front of the front wall to hold the chocolate pellets (#1811223, 20 mg, TestDiet) for reward. The food pellet was placed 0.7 cm away from the front wall and 0.4 cm away from the midline of the slit, to encourage the mouse to use the dominant hand for catching (Figure 1A). The task has two periods, shaping and training. Mice were food restricted to keep approximately 90% body weight of the original weight during the whole process (Figure1B). On shaping day one, two mice from the same cage were placed into the chamber for 20 min to acclimate to the environment; on shaping day two, an individual mouse was placed into the chamber for 20 min. During shaping, 10 food pellets were feed for each mouse every day to train mice eating food pellets. On shaping day 3, a food tray full of food pellets was placed in front of the middle slit. The mouse can get the food reward by catching it through the slit with either hand. The experiment stopped when 20 times of reaching attempts were finished for each mouse. The dominant hand should be the one that shows over 70% preference. During the training period, mice reached for food pellets through the slit by the dominant hand, 40 attempts within 20 min every day. Only

562 attempts by the dominant hand were counted. Based on the results of the attempts, the
563 reaching attempts show four types: miss, no-grasp, drop, and success. A "miss" means
564 that the hand does not touch the food pellet. A "no-grasp" means that the hand of the
565 mouse touches the food pellet, but it does not successfully grasp the pellet. A "drop"
566 represents the mouse grasps the pellet, but it dropped due to whatever reasons during
567 the retrieval. A "success" was a reach in which the mouse successfully retrieved the
568 pellet and put it into the mouth of the mouse. A high-speed camera was placed on the
569 side of the chamber to videotape the reaching behavior of mice at 60 frames per
570 second. The success rate was calculated as the number of successful attempts / the
571 total attempts. The miss rate, the no-grasp rate, and the drop rate were also calculated
572 to evaluate the performance of each step of mice. Hausdorff distances, the greatest of
573 all the distances from a point in one set to the closest point in the other set, were
574 calculated to assess the variation of trajectories.
575
576 ***CCKBR antagonist injection***
577 C57BL/6 mice were implanted a cannula in the motor cortex (coordinates: AP,1.4
578 mm, ML, -/+1.6 mm, DV, 0.2 mm) contralateral to the dominant hand of the mice,
579 followed by three days of recovery. Mice were grouped into antagonist and vehicle
580 groups. L365,260 (CCKBR antagonist) (1 ul, 20 uM, Cat. No. 2767, biotechne) or
581 vehicle (0.1% DMSO dissolved in ACSF) was injected into the motor cortex through
582 the cannula with the flow rate of 100 nl/ min pumped by a syringe pump (Hamilton,
583 USA), before the mice were placed into the chamber for the single pellet reaching

584 task training.

585

586 ***Chemogenetic manipulation***

587 A Chemogenetics experiment was performed on CCK-ires-Cre mice (#012706,
588 Jackson Laboratories). Cre-dependent hM4Di virus was injected into the rhinal cortex.
589 Detailed coordinates and volumes were described in the virus injection part. Mice
590 were used for single pellet reaching task training four weeks post virus injection.
591 Thirty minutes before behavior training, clozapine (0.4 mg/kg, Sigma-Aldrich,
592 dissolved with 0.1% DMSO) was intraperitoneally injected to inactivate the activity
593 of the CCK-expressing neurons in the rhinal cortex. The same volume of vehicle
594 (0.9% saline solution with 0.1% DMSO) was injected for the sham control group. A
595 negative control virus (AAV8-hSyn-DIO-mCherry) combined with intraperitoneal
596 clozapine injection was also carried out to exclude the influence of clozapine on
597 motor learning ability.

598

599 ***Virus injection and surgical process***

600 AAV8-hSyn-DIO-mchery, AAV8-hSyn-DIO-hM4Di-mCherry were diluted to the
601 titer around $5x10^{12}$ copies/ml and AAV_{retro}-EF1a-DIO-EYFP,
602 AAV-hSyn-CaMKII-GCaMP6s-SV40 were diluted to the titer around $1x10^{13}$
603 copies/ml and injected into the mouse cortex as previously described (Zhu and Roth,
604 2015; Tervo et al., 2016; Wu et al., 2020). The mice were anesthetized with
605 pentobarbital with their fur between two ears trimmed and fixed on a stereotactic

606 apparatus (RWD, China). Firstly, the head skin of the mouse was cleaned and
607 sterilized with 70% alcohol and removed to expose the skull totally. To accurately
608 locate the areas of interest, the head was adjusted between middle and lateral, and
609 anterior and posterior. In order to completely inactivate the rhinal cortex, two
610 injection sites per hemisphere were determined for virus injection using the following
611 coordinates: site 1: anteroposterior (AP), -3.52 mm from Bregma, mediolateral (ML),
612 3.57 mm, dorsoventral (DV), -3.33 mm from the brain surface; site 2: AP, -4.24 mm
613 from Bregma, ML, 3.55 mm, DV, -2.85 from the brain surface. Microinjections were
614 carried out using a microinjector (world precision instruments, USA) and a glass
615 pipette (Cat#504949, world precision instruments, USA). The volume is 200 nl for
616 each site and the flow rate is 50 nl/min.

617 To track the projection of CCK neuron from the rhinal cortex to the motor cortex,
618 retrograde AAV-EF1a-DIO-eYFP was injected into the motor cortex. The coordinates
619 is: site 1: AP, 1.8 mm to the Bregma, ML, 1.2 mm, DV 200 um, and 600 um; site 2:
620 AP, 1.0 mm to the Bregma, ML, 1.5 mm, DV, 200 um and 600 um. The volume of
621 each site at each DV was 200 nl and the flow rate was 20 nl/ min to protect the fluid
622 from flowing out. An anterograde AAV-hSyn-DIO-mCherry is also used for projection
623 tracking by injecting the virus into the rhinal cortex of the hemisphere. The specific
624 coordinates are as described above. After virus injection, skins were seamed with
625 sterilized sewing thread, and the cut was spread with antibiotic paste to protect it from
626 pathogens and accelerate healing.

627 The surface virus infusion process for the calcium imaging was performed as

628 described previously with mild modification (Li et al., 2017). A wide-tip glass pipette
629 was prepared by a micropipette puller and then cut, polished, and flame-treated to
630 make it even and smooth. Mice were intraperitoneally injected with dexamethasone
631 (0.2 mg/kg, s.c.) and carprofen (5 mg/kg, s.c.) to protect the brain from swelling and
632 inflammation. Three hours later, mice were anesthetized with pentobarbital. The
633 periosteum covered on the skull was removed, cleaned, and dried with 100% alcohol
634 to prevent the skull and tissues from growing. A 3 x 3 mm^2 window above the motor
635 cortex contralateral to the dominant hand was opened with a hand drill, and the bone
636 debris was carefully removed with fine forceps. After that, the dura around the
637 injection area was removed (open a dura hole of about 1 mm^2) to expose the pial
638 tissue for virus infusion. The tip of the pipette tightly covered the brain surface by
639 lowering 400-500 um, and 0.6 ul virus was infused at the speed of 0.06 ul/min. A 3 x
640 3 cover glass (thickness, around 150 um) was attached to the brain surface, and gentle
641 pressure was applied to keep the cover glass at the level same as the skull. The edge
642 of the cover glass was sealed with superglue. After the glue totally hastened, the skin
643 was stretched back and sutured.
644
645 ***Baseplate implantation***
646 2-3 weeks after cranial window implantation, the scalp over the skull was totally
647 removed with surgical scissors. Success implantation shows a clear observation
648 window without blood on the brain surface and a cover glass tightly fixed on the skull.
649 The cover glass surface was gently cleaned with Ringer's solution and lens paper, and

650 the regrowth of periosteum on the skull was removed with fine forceps. Before
651 baseplate implantation, the skull was dried with 100% alcohol, covered with Metbond
652 glue, and a thick layer of dental acrylic except for the cover glass for observation.
653 A one-photon miniscope (UCLA miniscope V4, Lab maker, Germany) connected to
654 the data acquisition software was attached to the baseplate, secured on the stereotaxic
655 micromanipulator, and gradually lowered to the cover glass until there was only a 1
656 mm gap between the skull and the baseplate. We turned on the LED and adjusted the
657 focal distance of the electrowetting lens to 0 on the software. The position of the
658 miniscope was adjusted until the brain tissue was observed in the data acquisition
659 system. Dental acrylic was used to fix the baseplate to the acrylic cap covering the
660 skull around the window. Once the dental acrylic had hardened, the miniscope was
661 removed, and a metal cap was attached to the baseplate to protect the cover glass
662 window.
663
664 ***Calcium imaging and fluorescent signal analysis***
665 After the implantation of the baseplate, a miniscope model was attached to the
666 baseplate, and the mouse was placed in the chamber to acclimate to the weight of the
667 miniscope for 20 minutes for 3 days. The LED laser and focal plate were slightly
668 adjusted until the cells with fluorescent protruded from the background. A web
669 camera was also connected to the data acquisition software and recorded the behavior
670 movement of the animal simultaneously.
671 An imaging field of about 1.0 x 1.0 mm^2 (resolution: 608 x 608 pixels) video at

672 approximately 10 min long was recorded. To clearly figure out the role of CCK
673 played in the neuronal plasticity of the motor cortex from $CCK^{-/-}$ mice, C57BL/6 mice
674 as well as C57BL/6 mice that intraperitoneal injection of CCKBR antagonist,
675 L365,260 (0.4 mg/kg, Cat. No. 2767, biotechne). Raw AVI videos were firstly
676 spatially down-sample by two folds to reduce the size of the videos by Fiji (Image J,
677 USA). Then a MATLAB algorithm, NoRMCorre, was applied for piecewise rigid
678 motion correction before data analysis. The calcium signals were extracted with the
679 MATLAB code of Constrained Nonnegative Matrix Factorization for
680 microEndoscopic (CNMF-E) (code availability: https://github.com/zhoupc/CNMF_E)
681 (Zhou et al., 2018). The scaled fluorescent calcium signal overtime was extracted as
682 C_raw. The raw data was then deconvolved. The activity higher than 3 times the
683 standard deviation of baseline fluctuation is deemed as a calcium event which has
684 been revealed to be associated with neuronal spiking activity, and the rising phase of
685 which was searched and used for further neuronal activity analysis (Peters et al., 2014;
686 Wang et al., 2017). Timestamps from both the behavior videos and the calcium
687 imaging videos were aligned to find out the time window when the mouse performed
688 the reaching task. Neuronal activity in the time window from 100 ms before reaching
689 to 100 ms after retrieval was considered the activity related to the movements.
690 Wilcoxon ranksum test was conducted between activity inside the time window and
691 activity outside ($p<0.05$) to exclude the neurons that activated indiscriminately or not
692 correlated with the reaching task. Neurons with the average activity in the time
693 window higher than the average outside the time window were considered

694 movement-related neurons. The neurons were aligned based on each neuron's sorted
695 time of peak event to visualize each and all the neuronal activity patterns during the
696 reaching task. The recurrence of neuronal activities related to the movements was also
697 elevated by pairwise comparison of the population neuronal activity between trials
698 using the Pearson correlation coefficient.

699

700 ***Immunohistochemistry***

701 Four weeks after virus injection, mice were perfused with 50 mL cold PBS buffer
702 (1x) to remove the blood and 50 mL 4% paraformaldehyde (PFA) in PBS to fix the
703 brain tissue. The skull was carefully opened, and the brain was removed from the
704 skull and fixed by immersing it in 4% PFA at 4 ^{o}C for 24 hours, then dehydrated in
705 30% sucrose PBS solution until it sank to the bottom. Brains were covered with OTC,
706 freezing fixed, and sectioned to a thickness of 50 um using a freezing microtome
707 (Leica, German). Brain slices were preserved in an anti-freezing solution (25%
708 glycerol and 30% ethylene glycol, in PBS) and stored in the -80 ^{o}C refrigerator.

709 For immunostaining, the brain slices were washed 3 times using 1 x PBS in a
710 shaker and incubated in blocking solution (10% normal goat serum and 0.2% Triton
711 X-100 in PBS) for more than 1.5 hours in a shaker and incubated with the primary
712 antibody (Mouse anti- GAD67, Millipore; Mouse anti-CaMK2a, Abcam; Mouse
713 anti-mCherry, Invitrogen) in 0.2% Triton and 5% Goat serum in PBS at 4 ^{o}C for 24
714 -36 hours. Slices were washed with PBS four times before incubating with the second
715 antibody (Alexa Fluor 594 conjugated goat anti-mouse, Alexa Fluor 594 conjugated

716 goat anti-rabbit, Jackson immunity) diluted in 0.1% Triton PBS solution for 3 hours.
717 Finally, slices were washed in 1 x PBS 4 times, then incubated with DAPI (1mg/ml)
718 for 10 min, mounted on slides and sealed with mounting medium (70% glycerol in
719 PBS). Slices were observed and imaged with a confocal laser-scanning microscope
720 (Zeiss, German) using 10 x and 20 x air objectives or 40 x and 60 x oil immersion
721 objectives.
722
723 ***Brain Slice Electrophysiology***
724 The slice electrophysiology experiment was carried out following the methods
725 reported previously (Chen et al., 2019). In the experiments, 6-8 weeks old C57BL/6
726 or $CCK^{-/-}$ mice were anesthetized with isoflurane in a small chamber. The mouse head
727 was cut, and the brain was rapidly removed and put into an oxygenated (95% O_2-5%
728 CO_2) artificial cerebral spinal fluid (ACSF) cold bath containing 26 mM of $NaHCO_3$,
729 2 mM of $CaCl_2$, 1.25 mM of KH_2PO_4, 1.25 mM of $MgSO_4$, 124 mM of NaCl, 3 mM
730 of KCl and 10 mM of glucose, pH 7.35–7.45. The brain was sectioned from the
731 middle line into two hemispheres. The portions with the brain areas of the motor
732 cortex were trimmed and glued on the ice-cold stage of a vibrating tissue slicer (Leika
733 VT1000S). Coronal sections of slices containing the motor cortex (300 μm thick)
734 were trimmed and gently transferred into an ACSF containing chamber, which was
735 put in a water bath at 28 °C and oxygen blowing continuously. After 2 hours of
736 recovery in the ACSF bath, the slice was applied for the following
737 electrophysiological recording.

738 A commercial 4-slice 8 x 8 channels recording system (MED, Panasonic
739 Alpha-Med Sciences) was applied to record the fEPSPs. The MED probe is composed
740 of 64 microelectrodes; the distance between the two channels is 50 x 50 μm,
741 (MED-P515A, 64-channel, 8 x 8 pattern, 50 x 50 um, inter-electrode distance 150 μm
742 or MED-PG515A).

743 After recovery, the motor cortex slice was covered by the recording electrodes. A
744 fine-mesh anchor (Warner Instruments, Harvard) was covered on the brain slice to
745 stabilize it, and the probe chamber was perfused with fresh ACSF oxygenated with
746 oxygen with a peristaltic pump (Minipuls 3, Gilson), and the water bath was kept at
747 32 °C. After 20 min of recovery, one of the microelectrodes in the area of interest was
748 selected as the stimulating electrode through an inverted camera (DP70, Olympus).
749 The surface layer of the motor cortex was stimulated with constant current pulses at
750 0.1 ms in duration at 0.017 Hz by the connected controlling software, data acquisition
751 software (Mobius, Panasonic Alpha-Med Sciences). After the baseline recording,
752 which was stimulated at the currency of that triggering around 50% of the saturating
753 potential. For drug application, CCK4 (final concentration: 500 nM) or vehicle was
754 injected into the electrode dishes. High-frequency stimulation (HFS) (25 bursts at 120
755 Hz for each burst, at the highest intensity) was applied to the simulation probe. The
756 electrophysiological data were extracted and analyzed with offline software, Mobius
757 software. For quantification of the LTP data, the initial amplitudes of fEPSPs were
758 normalized and expressed as percentage changes over the averaged baseline activity.
759 The fEPSP was normalized based on the percentage of the baseline potential.

760

761 ***Rescue of the motor learning ability of the CCK$^{-/-}$ mice with CCK4***

762 CCK4, a tetrapeptide derived from the peptide of CCK was selected as a potential
763 drug to rescue the motor learning defect caused by the lack of CCK, because CCK4
764 remains the function to activate the CCK receptor but has a much smaller molecule
765 than CCK8s or CCK58, making it transmit through the brain-blood barrier easily and
766 smoothly (Javanmard et al., 1999; Eser et al., 2009). Therefore, intraperitoneal
767 injection of the CCK4 is a simple and easily available way to rescue CCK lack caused
768 motor learning defects.

769 After shaping, CCK$^{-/-}$ mice were injected intraperitoneally with CCK4 (0.45 mg/kg,
770 Cat# ab141328, Abcam, UK) or vehicle before training every day.

771

772 ***Statistical analysis***

773 Group data were shown as mean ± SEM (standard error of the mean) unless
774 otherwise stated. Statistical analyses, including paired t-tests, one-way RM ANOVA,
775 and two-way mixed ANOVA, were conducted in SPSS 26 (IBM, Armonk, NY).
776 Statistical significance was defined as $p < 0.05$ by default.

777

778 **Data availability**

779 Data for this submission has been uploaded to the Dryad Digital Repository,
780 https://doi.org/10.5061/dryad.9ghx3ffms.

781

ACKNOWLEDGMENTS

We thank Eduardo Lau and Friday for administrative and technical assistance.We also thank the following charitable foundations for their generous support to JFH: Wong Chun Hong Endowed Chair Professorship, Charlie Lee Charitable Foundation.

Funding: This work was supported by: Hong Kong Research Grants Council, General Research Fund (GRF, 11103220M and 11101521M); Hong Kong Research Grants Council, Collaborative Research Fund (C7048-16g); Innovation and Technology Fund (MRP/053/18X, GHP_075_19GD); Health and Medical Research Fund (HMRF, 09203656); National Natural Science Foundation of China (NSFC, 31671102).

Competing Interest Statement

No competing interest exits in the submission of this manuscript.

804 **Reference**

805 Ackermann S, Rasch B (2014) **Differential effects of non-REM and REM sleep on**
806 **memory consolidation?** *Curr Neurol Neurosci Rep*, 14(2),430.
807 https://doi.org/10.1007/s11910-013-0430-8.

808 Aydin OU, Taha AA, Hilbert A, Khalil A A, Galinovic I, Fiebach JB, Madai VI (2021)
809 **On the usage of average Hausdorff distance for segmentation performance**
810 **assessment: hidden error when used for ranking** *Euro. Radiol. Exp.* 5(1), 1-7.
811 https://doi.org/10.1186/s41747-020-00200-2.

812 Bandopadhyay R, Belleroche De J (1991) **Regulation of CCK release in cerebral**
813 **cortex by N-methyl-D-aspartate receptors: Sensitivity to APV, MK-801,**
814 **kynurenate, magnesium and zinc lons** *Neuropeptides* 18(3), 159-163.
815 https://doi.org/10.1016/0143-4179(91)90108-U.

816 Biane JS, Takashima Y, Scanziani M, Conner JM, Tuszynski MH (2016)
817 **Thalamocortical projections onto behaviorally relevant neurons exhibit plasticity**
818 **during adult motor learning** *Neuron* 89(6), 1173-1179.
819 https://doi.org/10.1016/j.neuron.2016.02.001.

820 Brigard De F (2019) **Know-how, intellectualism, and memory systems** *Philos.*
821 *Psychol.* 32(5), 719-758.
822 https://doi.org/10.1080/09515089.2019.1607280.

823 Chen CC, Gilmore A, Zuo Y (2014) **Study Motor skills learning by Single-pellet**

824 **Reaching Tasks in Mice** *J. Vis. Exp*. (85), e51238.

825 https://doi.org/10.3791/51238.

826 Chen SX, Kim AN, Peters AJ, Komiyama T (2015) **Subtype-specific plasticity of**
827 **inhibitory circuits in motor cortex during motor learning** *Nat. Neurosci.* 18,
828 1109–1115.

829 https://doi.org/10.1038/nn.4049.

830 Chen X, Guo Y, Feng J, Liao Z, Li X, Wang H, He J (2013) **Encoding and retrieval**
831 **of artificial visuoauditory memory traces in the auditory cortex requires the**
832 **entorhinal cortex** *J. Neurosci*. 33(24), 9963-9974.

833 https://doi.org/10.1523/JNEUROSCI.4078-12.2013.

834 Chen X, Li X, Wong YT, Zheng X, Wang H, Peng Y, He J (2019) **Cholecystokinin**
835 **release triggered by NMDA receptors produces LTP and sound-sound associative**
836 **memory** *Proc. Natl. Acad. Sci. U.S.A.* 116(13), 6397-6406.

837 https://doi.org/10.1073/pnas.1816833116.

838 Cheney PD (1985) **Role of cerebral cortex in voluntary movements: A review**
839 *Physical Therapy* 65(5), 624-635.

840 https://doi.org/10.1093/ptj/65.5.624.

841 Corkin S (1968) **Acquisition of motor skill after bilateral medial temporal-lobe**
842 **excision** *Neuropsychologia* 6(3), 255-265.

843 https://doi.org/10.1016/0028-3932(68)90024-9.

844 Costa RM, Cohen D, Nicolelis MA (2004) **Differential corticostriatal plasticity**
845 **during fast and slow motor skills learning in mice** *Curr. Biol.* 14, 1124–1134.
846 https://doi.org/10.1016/j.cub.2004.06.053.

847 Crawley JN, Corwin RL (1994) **Biological actions of cholecystokinin** *Peptides* 15(4),
848 731-755.
849 https://doi.org/10.1016/0196-9781(94)90104-X.

850 Economo MN, Viswanathan S, Tasic B, Bas E, Winnubst J, Menon V, Svoboda K
851 (2018) **Distinct descending motor cortex pathways and their roles in movement**
852 *Nature* 563(7729), 79-84.
853 https://doi.org/10.1038/s41586-018-0642-9.

854 Eser D, Leicht G, Lutz J, Wenninger S, Kirsch V, Schüle C, Mulert C (2009)
855 **Functional neuroanatomy of CCK-4-induced panic attacks in healthy volunteers**
856 *Hum. Brain Mapp*. 30(2), 511-522.
857 https://doi.org/10.1002/hbm.20522.

858 Feng H, Su J, Fang W, Chen X, He J (2021) **The entorhinal cortex modulates trace**
859 **fear memory formation and neuroplasticity in the mouse lateral amygdala via**
860 **cholecystokinin** *Elife* 10, e69333. https://doi.org/10.7554/eLife.69333.

861 Heindorf M, Arber S, Keller GB (2018) **Mouse motor cortex coordinates the**
862 **behavioral response to unpredicted sensory feedback** *Neuron* 99(5), 1040-1054.
863 https://doi.org/10.1016/j.neuron.2018.07.046.

Hooks BM, Mao T, Gutnisky DA, Yamawaki N, Svoboda K, Shepherd GM (2013) **Organization of cortical and thalamic input to pyramidal neurons in mouse motor cortex** J. Neurosci. 33(2), 748-760.

https://doi.org/10.1523/JNEUROSCI.4338-12.2013.

Hosp JA, Pekanovic A, Rioult-Pedotti MS, Luft AR (2011) **Dopaminergic projections from midbrain to primary motor cortex mediate motor skills learning** *J. Neurosci.* 31, 2481-2487.

https://doi.org/10.1523/JNEUROSCI.5411-10.2011.

Huber D, Gutnisky DA, Peron S, O'connor H, Wiegert JS, Tian L, Svoboda K (2012) **Multiple dynamic representations in the motor cortex during sensorimotor learning** *Nature* 484(7395), 473-478.

https://doi.org/10.1038/nature11039.

Javanmard M, Shlik J, Kennedy SH, Vaccarino FJ, Houle S, Bradwejn J (1999) **Neuroanatomic correlates of CCK-4-induced panic attacks in healthy humans: a comparison of two time points** *Biol. Psychiatry* 45(7), 872-882.

https://doi.org/10.1016/S0006-3223(98)00348-5.

Li X, Cao VY, Zhang W, Mastwal SS, Liu Q, Otte S, Wang KH (2017) **Skin suturing and cortical surface viral infusion improves imaging of neuronal ensemble activity with head-mounted miniature microscopes** *J. Neurosci. Methods.* 291, 238-248.

884 https://doi.org/10.1016/j.jneumeth.2017.08.016.

885 Li X, Yu K, Zhang Z, Sun W, Yang Z, Feng J, He J (2014) **Cholecystokinin from the**
886 **entorhinal cortex enables neural plasticity in the auditory cortex** *Cell Res.* 24(3),
887 307-330.
888 https://doi.org/10.1038/cr.2013.164.

889 Meunier M, Hadfield W, Bachevalier J, Murray EA (1996) **Effects of rhinal cortex**
890 **lesions combined with hippocampectomy on visual recognition memory in rhesus**
891 **monkeys** *J. Neurophysio.* 75(3), 1190-1205.

892 https://doi.org/10.1152/jn.1996.75.3.1190.

893 Papale AE, Hooks BM (2018) **Circuit changes in motor cortex during motor skills**
894 **learning** *Neurosci. Rev.* 368, 283 - 297.
895 https://doi.org/10.1016/j.neuroscience.2017.09.010.

896 Peters AJ, Chen SX, Komiyama T (2014) **Emergence of reproducible**
897 **spatiotemporal activity during motor learning** *Nature* 510, 263–267.
898 https://doi.org/10.1038/nature13235.

899 Peters AJ, Lee J, Hedrick NG, O'Neil K, Komiyama T (2017) **Reorganization of**
900 **corticospinal output during motor learning** *Nat. Neurosci*. 20(8), 1133-1141.
901 https://doi.org/10.1038/nn.4596.

902 Sanes JN, Donoghue JP (2000) **Plasticity and primary motor cortex** *Annu. Rev.*
903 *Neurosci.* 23(1), 393-415.

https://www.annualreviews.org/doi/10.1146/annurev.neuro.23.1.393.

Schindelin J, Arganda-Carreras I, Frise E, Kaynig V, Longair M, Pietzsch T, Preibisch S, Rueden C, Saalfeld S, Schmid B, Tinevez JY, White DJ, Hartenstein V, Eliceiri K, Tomancak P, Cardona A (2012) **Fiji: an open-source platform for biological-image analysis** *Nature Methods* **9**:676–682.
https://doi.org/10.1038/nmeth.2019.

Squire LR (2004) **Memory systems of the brain: a brief history and current perspective** *Neurobiol. Learn Mem*. 82(3), 171-7.
https://doi.org/10.1016/j.nlm.2004.06.005.

Su J, Ye W, Liu H, Zhang B, Jendrichovsky P, Hoang AD, Chen X, Lau CYG, Yu D, Xiong W, Tortorella M, He J (2019) **Entorhinal cholecystokinin enables theta-burst stimulation-induced hippocampal LTP and transfer of spatial memory** *Neuron*
10.2139/ssrn.3451411.
https://doi.org/10.2139/ssrn.3451411.

Svoboda K, Li N (2018) **Neural mechanisms of movement planning: motor cortex and beyond** *Curr. Opin. Neurobiol.* 49, 33-41.
https://doi.org/10.1016/j.conb.2017.10.023.

Tervo DGR, Hwang BY, Viswanathan S, Gaj T, Lavzin M, Ritola KD, Karpova AY (2016) **A designer AAV variant permits efficient retrograde access to projection neurons** *Neuron* 92(2), 372-382.
https://doi.org/10.1016/j.neuron.2016.09.021.

Wagner MJ, Savall J, Hernandez O, Mel G, Inan H, Rumyantsev O, Schnitzer MJ

(2021) **A neural circuit state change underlying skilled movements** *Cell* 184(14), 3731-3747. https://doi.org/10.1016/j.cell.2021.06.001.

Wang X, Liu Y, Li X, Zhang Z, Yang H, Zhang Y, He Z (2017) **Deconstruction of corticospinal circuits for goal-directed motor skills** *Cell* 171(2), 440-455. https://doi.org/10.1016/j.cell.2017.08.014.

Wank SA (1995) **Cholecystokinin receptors** *Am. J. Physiol*. 269(5), G628-G646. https://doi.org/10.1152/ajpgi.1995.269.5.G628.

Watakabe A, Hirokawa J, Ichinohe N, Ohsawa S, Kaneko T, Rockland KS, Yamamori T (2012) **Area-specific substratification of deep layer neurons in the rat cortex** *J. Comp. Neuro.* 520(16), 3553-3573. https://doi.org/10.1002/cne.23160.

Wu HG, Miyamoto YR, Castro LNG, Ölveczky BP, Smith MA (2014) **Temporal structure of motor variability is dynamically regulated and predicts motor learning ability** *Nat. Neurosci.* 17(2), 312-321. https://doi.org/10.1038/nn.3616.

Xu T, Yu X, Perlik AJ, Tobin WF, Zweig JA, Tennant K, Zuo Y (2009) **Rapid formation and selective stabilization of synapses for enduring motor memories** *Nature* 462(7275), 915-919. https://doi.org/10.1038/nature08389.

947 Yaksh TL, Furui T, Kanawati IS, Go VLW (1987) **Release of cholecystokinin from**
948 **rat cerebral cortex in vivo: role of GABA and glutamate receptor systems** *Brain*
949 *Res.* 406(1-2), 207-214.

950 https://doi.org/10.1016/0006-8993(87)90784-0.

951 Zhou P, Resendez SL, Rodriguez-Romaguera J, Jimenez JC, Neufeld SQ,
952 Giovannucci A, Paninski L (2018) **Efficient and accurate extraction of in vivo**
953 **calcium signals from microendoscopic video data** *Elife* 7, e28728.

954 https://doi.org/10.7554/eLife.28728.

955 Zhu H, Roth BL (2015) **DREADD: a chemogenetic GPCR signaling platform** *Int. J.*
956 *Neuropsychopharmacology* 18(1).

957 https://doi.org/10.1093/ijnp/pyu007.

958

959

960

961

962

963

964

965

966

967

Figures

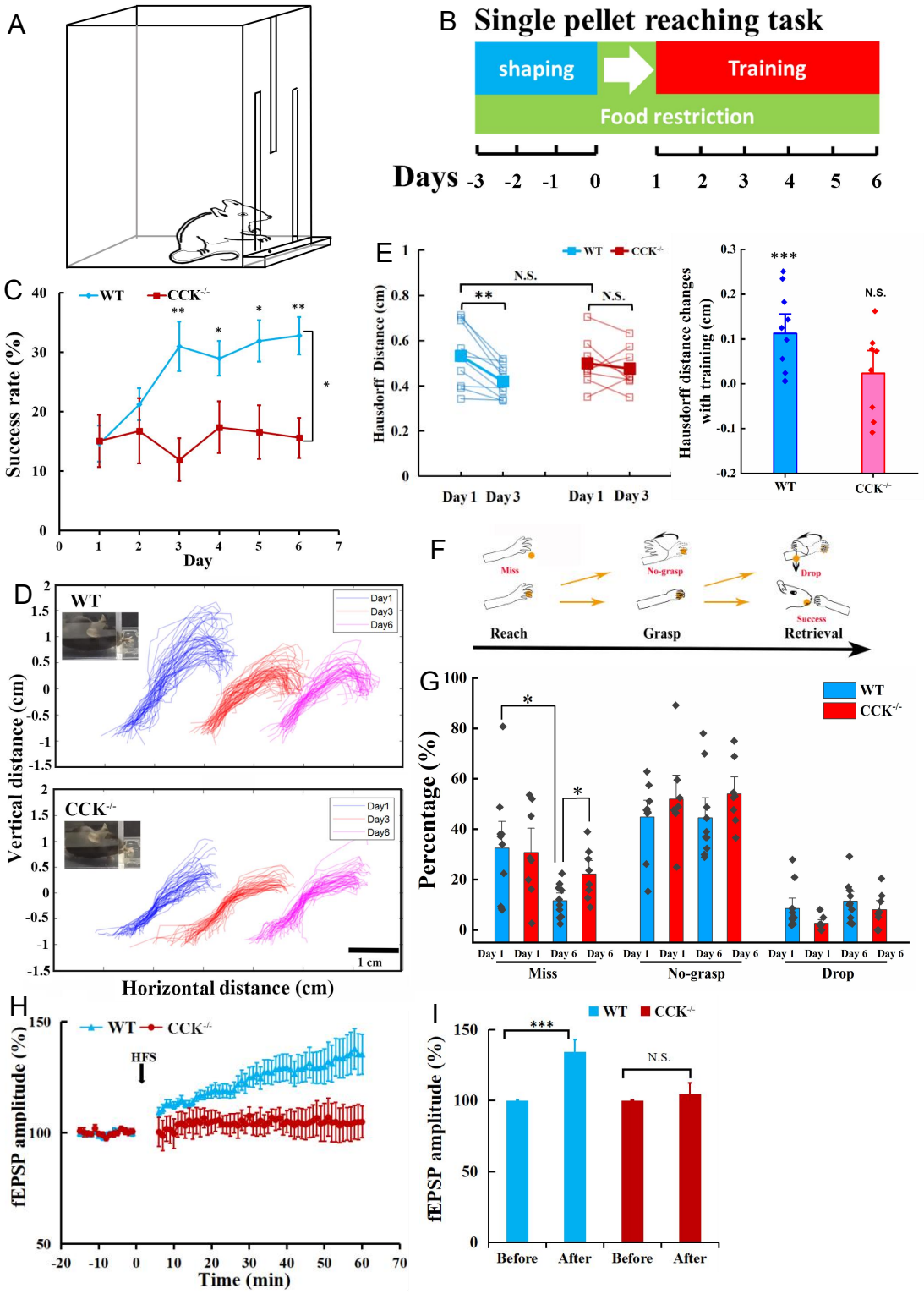

Figure 1. Single pellet reaching task for CCK$^{-/-}$ and WT mice. (A) Task schematic. A mouse reaches for the food pellet through the slit. (B) Procedure. Three days before training, the mouse was placed in the chamber and allowed to acclimate to the environment and determine the dominant hand. Throughout the procedure, the mouse was food restricted, keeping the body weight at approximately 90% of the original weight. (C) Success rate of wildtype (WT, C57BL/6) (N = 10) and CCK$^{-/-}$ (N = 8) mice performing the single pellet reaching task. *p<0.05, **p<0.01. Two-way mixed ANOVA, post hoc. comparison between two groups. (D) Representative trajectories of WT and CCK$^{-/-}$ mice at Day 1, Day 3, Day 6. (E) The pairwise Hausdorff distances of the trajectories were calculated to compare the variation in the trajectories of WT (N =10) and CCK$^{-/-}$ mice (N = 8). Left, blue and red solid square represent for average of the Hausdorff distance of WT and CCK$^{-/-}$ mice, respectively. **p<0.01, N.S. means not significant. Paired t-test. Right, Hausdorff distance changes with 3-day training of WT and CCK$^{-/-}$ mice. ***p<0.001, N.S. means not significant. t-test. (F) Diagram shows the task phases (reach, grasp, and retrieval) and different reaching results (miss, no-grasp, drop, and success). (G) Detailed reaching results for WT and CCK$^{-/-}$ mice on experimental Day 1 and Day 6. *p<0.05; paired t-test and t-test. (H) Normalized field EPSP amplitude before and after high frequency stimulation (HFS) for both WT (N = 6, n = 21) and CCK$^{-/-}$ mice (N = 3, n = 7). (I) The average normalized fEPSP amplitude 10 min before HFS (-10 - 0 min, before) and 10 min after HFS (50 – 60 min, after) in the two groups of mice. ***p<0.001, N.S. means not significant. Two-way mixed ANOVA, pairewise comparison.

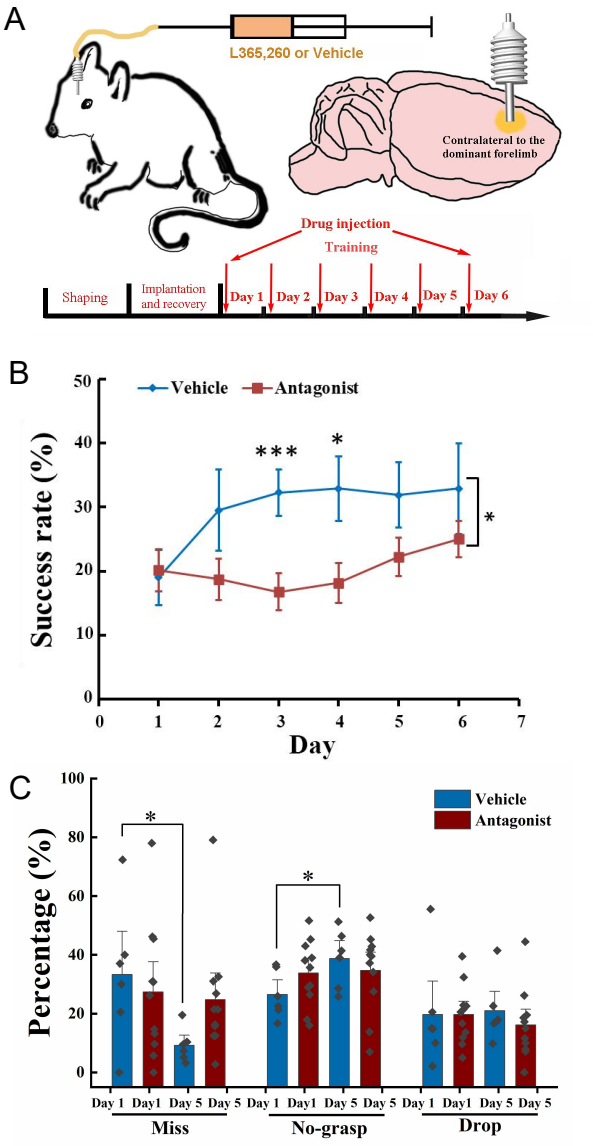

Figure 2. Effect of local injection of CCKBR antagonist on motor learning. (A) A cannula was implanted into the motor cortex contralateral to the dominant hand. One microliter of L365,260 or vehicle was injected into the motor cortex through the cannula every day before training. (B) Success rate of the mice injected with CCKBR antagonist (N = 11) and vehicle (N = 6). *p<0.05, ***p<0.001.Two-way mixed ANOVA, post hoc. comparison between two groups. (C) Detailed reaching results, in terms of miss, no-grasp, drop, on Day 1 and Day 5 for mice injected with CCKBR antagonist and vehicle. *p<0.05, paired t-test.

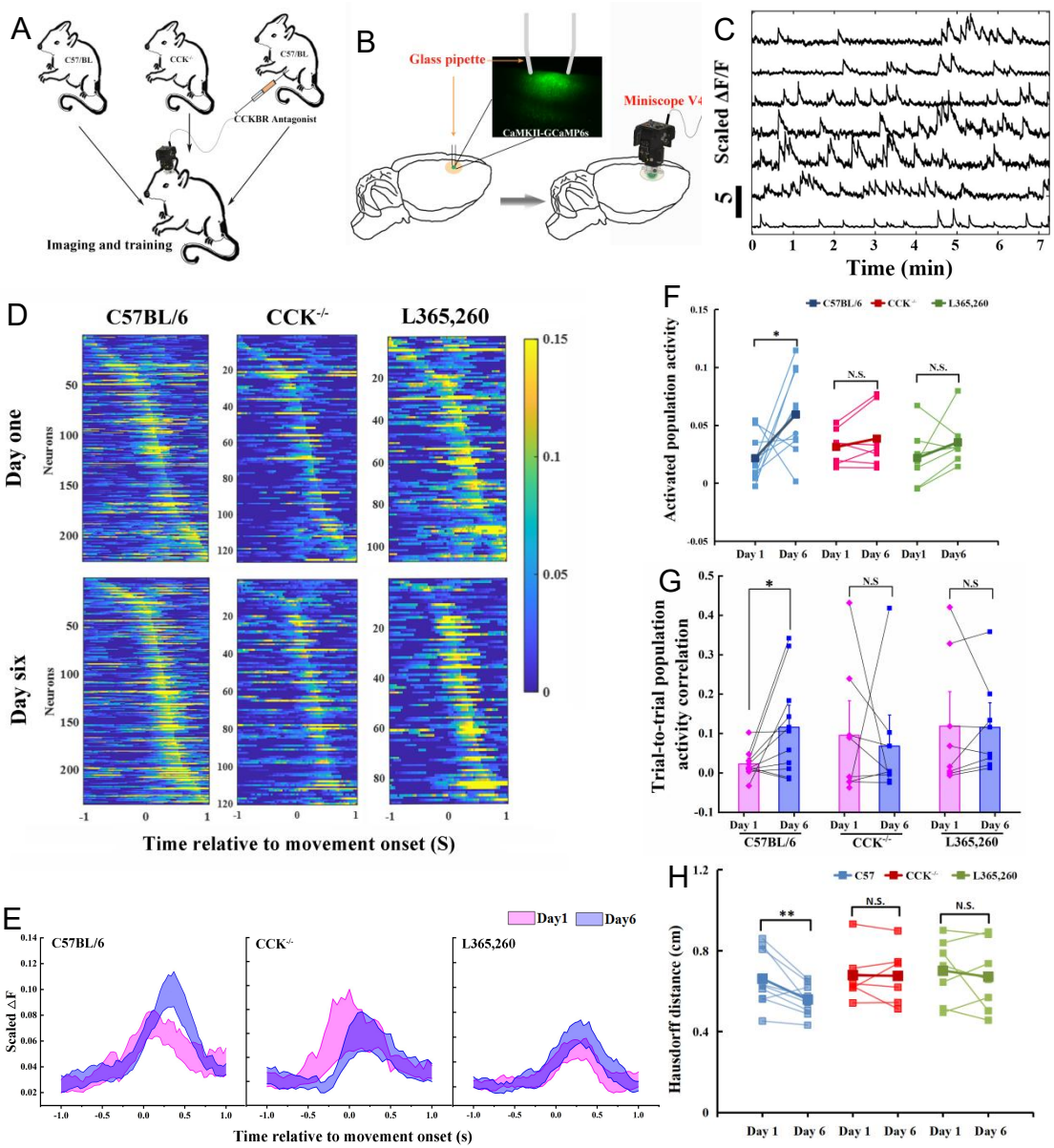

Figure 3. Calcium imaging of the MC during motor skill learning. (A) Experiment set-up. C57BL/6, CCK$^{-/-}$ and C57BL/6 mice injected with CCKBR antagonist were applied for single pellet reaching task training and calcium imaging. (B) Schematic diagram of calcium imaging. A wide-tip glass pipette tightly touched the brain by being lowered to a depth of 400-500 μm, and strong GCaMP6s virus expression was observed in the superficial layer of the motor cortex with a high contrast compared with the deep layers after >14 days of expression. A baseplate was implanted on the skull, which was connected to the miniscope for calcium imaging during motor skills training (right panel). (C) Representative traces of extracted neurons from miniscope using the CNMF-E algorithm. The scale bar represents 5 units of the scaled $\Delta F/F$ (D) Neuronal activity pattern of C57BL/6 (N = 10), CCK$^{-/-}$ (N = 7) and C57BL/6 mice injected with L365,260 (N = 7). Upper line is from training Day 1 and the bottom is from training Day 6. (E) Neuronal population activities from C57BL/6, CCK$^{-/-}$ and C57BL/6 mice injected with L365,260. (F) Activated population activity (peak activity minus baseline activity) was calculated for C57BL/6, CCK$^{-/-}$ and C57BL/6 mice injected with L365,260 at Day 1 and Day 6. *$p<0.05$, N.S. not significant. Paired t-test. (G) Trial-to-trial population activity correlation at Day 1 and Day 6 for C57BL/6, CCK$^{-/-}$ and C57BL/6 injected with L365,260. (H) The pairwise Hausdorff distances of the trajectories for C57BL/6, CCK$^{-/-}$ and C57BL/6 injected with L365,260 at Day 1 and Day 6. *$p<0.05$, N.S. not significant. One-way RM ANOVA.

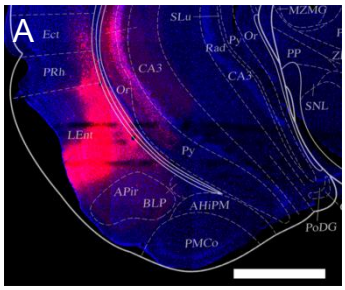

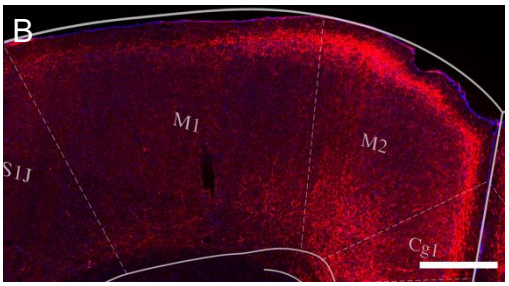

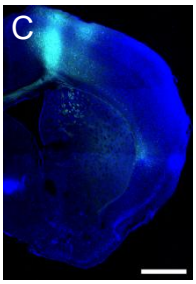

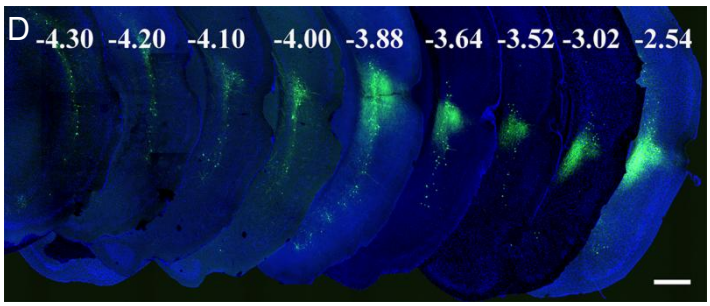

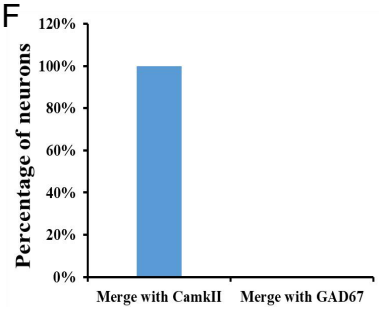

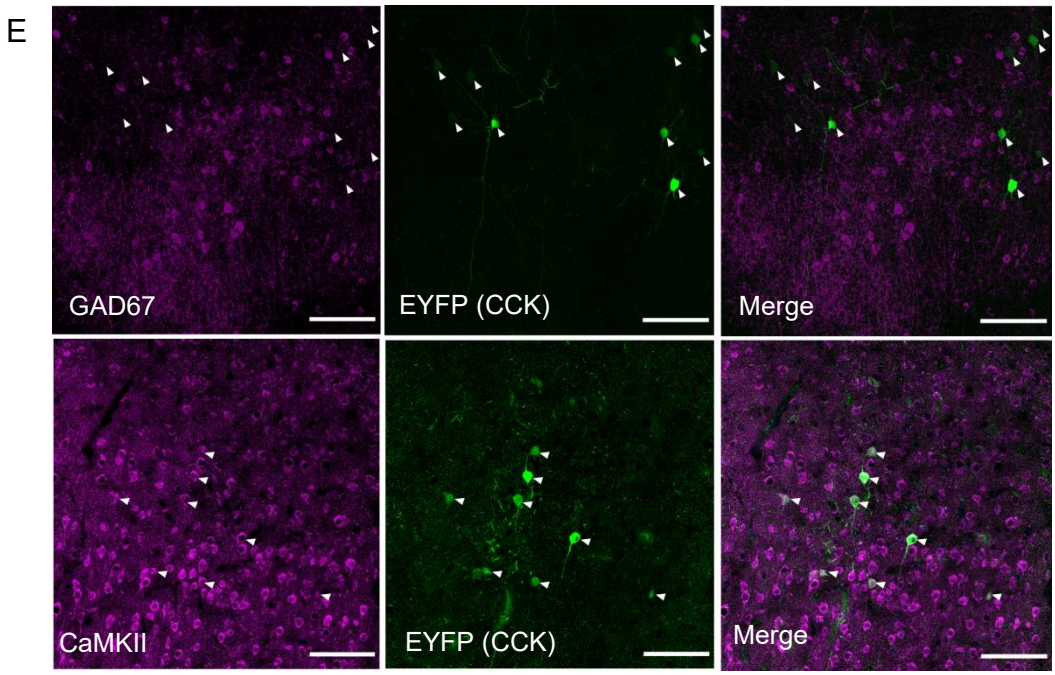

Figure 4. Labeling of CCK neuron projections from the RC to the MC. (A) Coronal section showing the virus injection site. The Cre-dependent AAV-hsyn-DIO-mCherry virus was injected into CCK-Cre mice. (B) Effective labeling of CCK neuron fibers in the MC. (C) Cre-dependent retrograde AAV virus injection site in the MC of the CCK-Cre mouse. (D) Continuous coronal brain sections showing EYFP in the lateral EC. The numbers (mm) indicate the position of the sections relative to the bregma. (E) GAD67 staining did not merge with the retrograde tracking CCK positive neurons in the EC and CaMKII staining merged with the signal of retrograde tracking CCK neurons EC projecting. Arrowhead indicate the positions of CCK neurons. (F) Percentage of retrogradely labeled neurons merged with CaMKII and GAD67 (n = 3). Scale bars represent 1000 μm in (A), (B), (C), and (D) and 100 μm in (E)

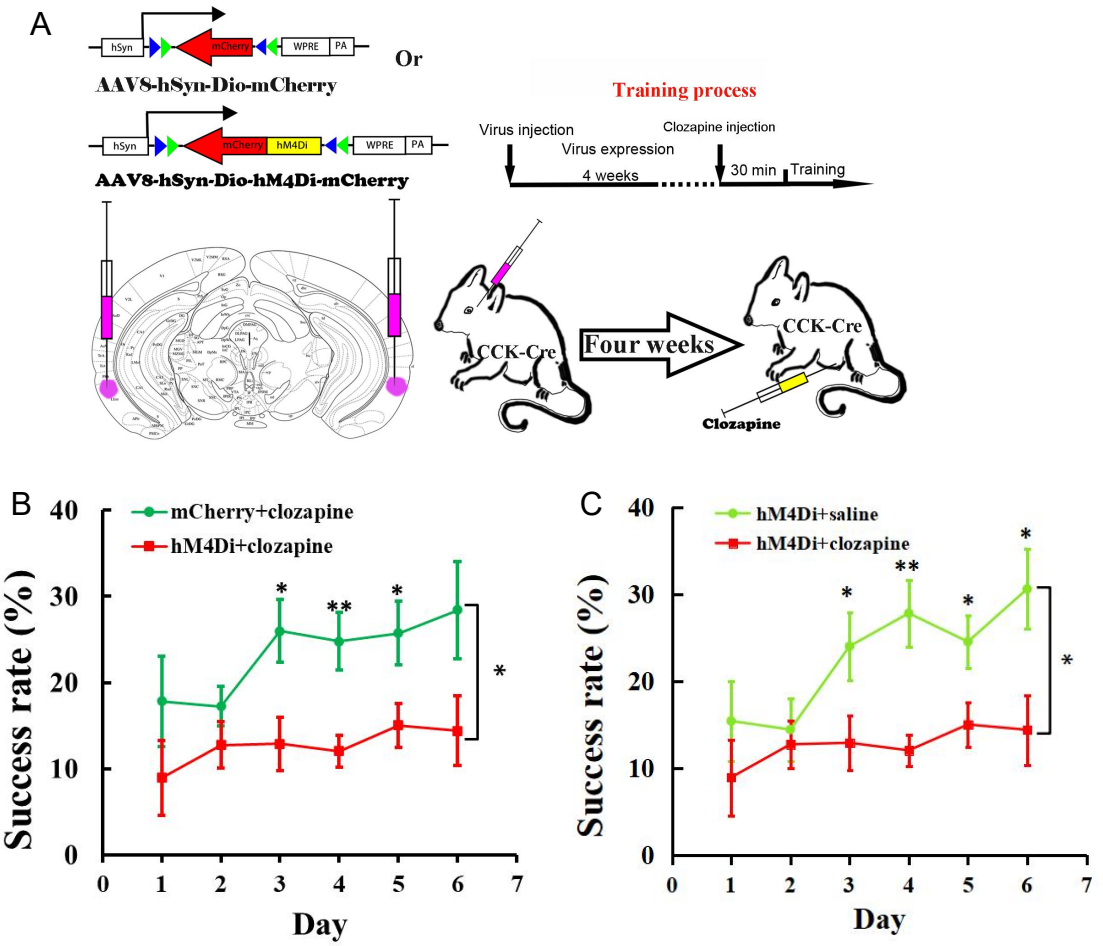

Figure 5. Effect of inhibition of the RC CCK neurons on motor learning. (A) Experimental paradigm for the chemogenetic experiment. Cre-dependent AAV-DIO-hM4Di-mCherry or AAV-DIO-mCherry was infused into the rhinal cortex of CCK-Cre mice. After four weeks, clozapine or saline was intraperitoneally injected 30 min before training. (B) Success rate of CCK-Cre mice injected with hM4Di containing virus plus clozapine (hM4Di+clozapine) (N = 10) and control virus plus clozapine (mCherry+clozapine) (N = 8).(C) Success rate of CCK-Cre mice injected with hM4Di containing virus plus clozapine (hM4di+clozapine, shared with B) and hM4Di plus saline (hM4Di+saline) (N = 11). The hM4Di+clozapine curve in Figure 5C shared that in B). *p<0.05, **p<0.01. Two-way mixed ANOVA, post hoc. comparison between two groups on different days.

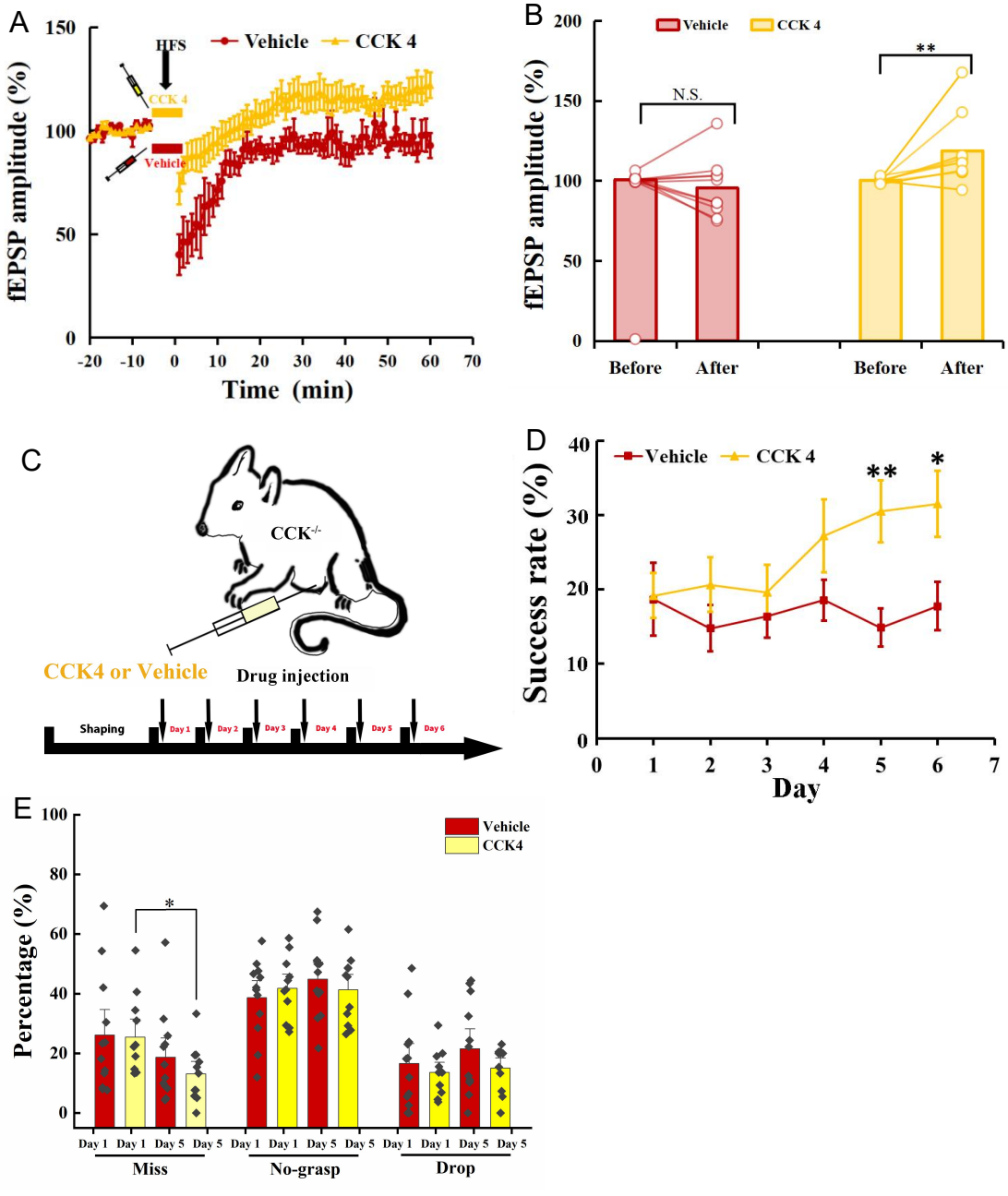

Figure 6. Rescuing the motor learning ability of CCK$^{-/-}$ mice by CCK 4. (A) Normalized fEPSP amplitude before and after HFS of the MC of CCK$^{-/-}$ mice applied with CCK4 (N = 6, n = 14) or vehicle (N = 6, n = 11). (B) The average normalized fEPSP amplitude 10 min before HFS (−10–0 min, before) and 10 min after HFS (50–60 min, after) in the MC of CCK$^{-/-}$ mice injected with CCK 4 or vehicle. *p<0.05, **p<0.01. Two-way mixed ANOVA with Bonferroni pairwise comparison. (C) Experimental paradigm for CCK rescuing experiment. CCK4 or vehicle was injected (i.p.) every day before training. (D) Success rate of CCK$^{-/-}$ mice injected with CCK4 (N = 11) or vehicle (N = 10). *p<0.05, **p<0.01. Two-way mixed ANOVA, post hoc. comparison between two groups on Day 5 and Day 6. (E) Detailed reaching results or CCK$^{-/-}$ mice injected (i.p.) with vehicle and CCK4 on Day 1 and Day 5. *p<005, N.S. not significant. Paired t-test.

Cholecystokinin from the Rhinal Cortex Facilitates Motor Skill Learning

Hao Li [a,b], Jingyu Feng[a], Mengying Chen[a], Min Xin[a,b], Xi Chen[a], Kuan Hong Wang[c,*], Jufang He[a,b,*]

[a] *Departments of Neuroscience and Biomedical Sciences, City University of Hong Kong, China.*

[b] *Centre for Regenerative Medicine and Health, Hong Kong Institute of Science & Innovation, Chinese Academy of Sciences, China.*

[c] *Department of Neuroscience, Del Monte Institute for Neuroscience, University of Rochester Medical Center, USA.*

[*] **Correspondence at**: Jufang He, Email: jufanghe@cityu.edu.hk; Kuan Hong Wang, Email: kuanhong_wang@urmc.rochester.edu.

Author Contributions: Jufang He, Kuan Hong Wang, Hao Li and Jingyu Feng designed the research; Hao Li, Jingyu Feng, and Xi Chen set up behavior model and analysis methods; Hao Li, Mengying Chen and Min Xin carried out the experiments; Hao Li, Xi Chen, Jufang He and Kuan Hong Wang analyzed the data; Hao Li and Jufang He wrote the draft of the manuscript; Hao Li, Jufang He and Kuan Hong Wang edited the manuscript.

Figure S1. Learning curve of single mouse of CCK$^{-/-}$ (A) and Wildtype (B) group

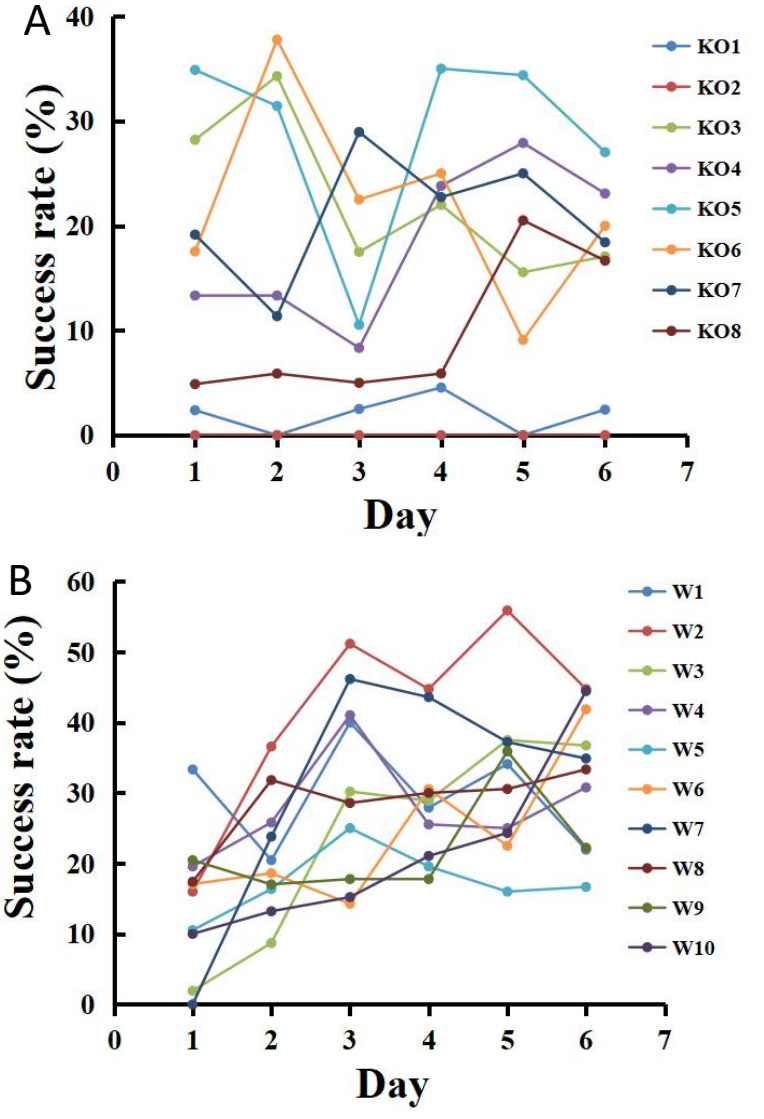

Figure S2. Learning curve of single mouse administrated with CCKBR Antagonist (A) and Vehicle (B).

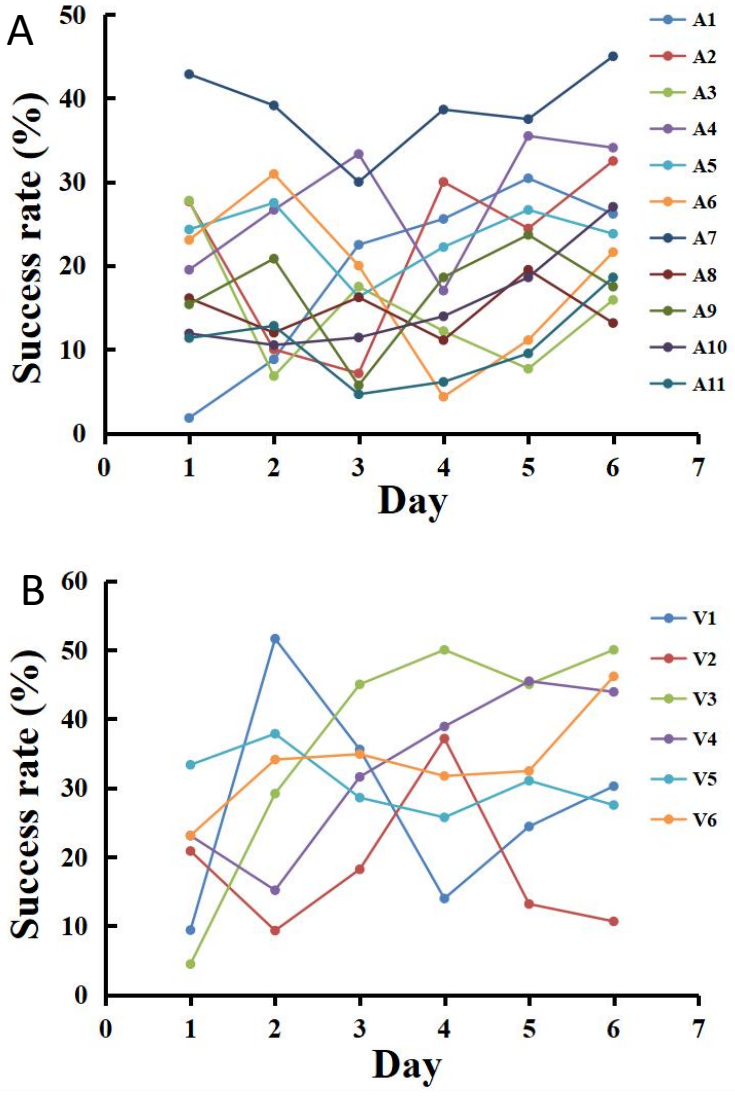

Figure S3. Neuronal activity related to the movement of different groups, including C57BL/6 (A, B), CCK$^{-/-}$ (C, D) and L365,260 injection (E, F) mice at Day 1 and Day 6.

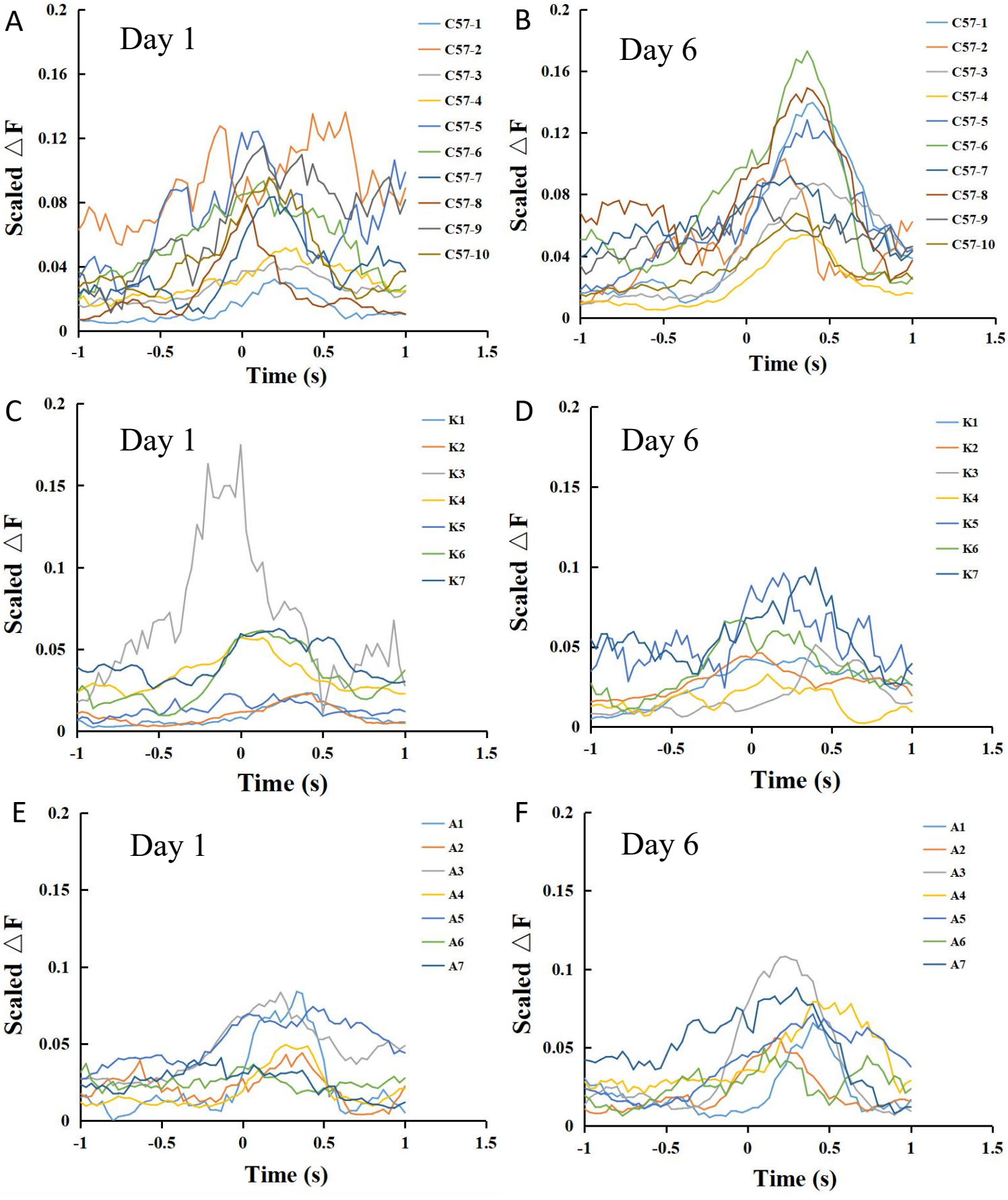

Figure S4. Learning curve of single CGK Cre mouse injected with hM4Di-clozapine (A), Control-clozapine (B) and hM4Di-saline (C).

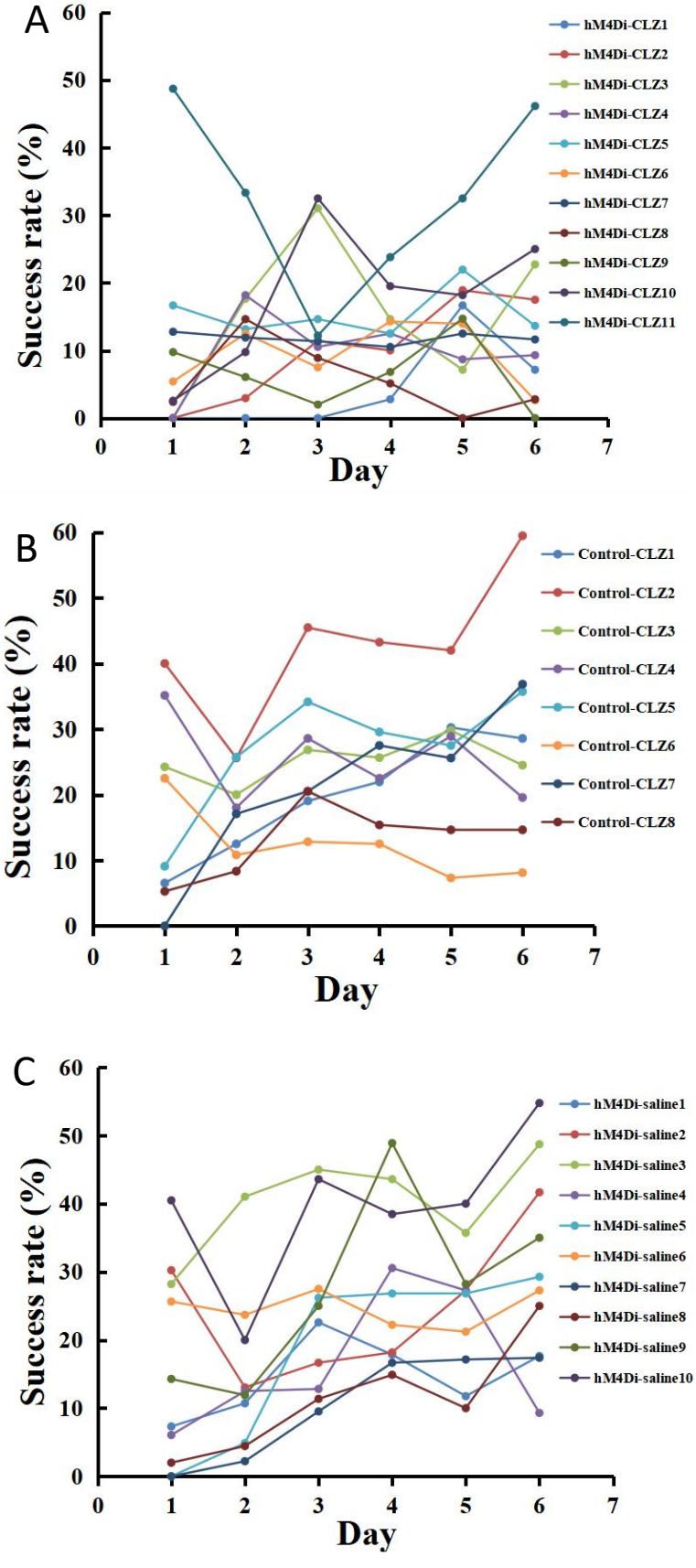

Figure S5. Learning curve of single CCK$^{-/-}$ mouse administrated with Vehicle (A) and CCK4 (B).